A Stochastic Model for The Transmission Dynamics of Toxoplasma Gondii

Guangyue Gao

Thesis submitted to the Faculty of the
Virginia Polytechnic Institute and State University
in partial fulfillment of the requirements for the degree of

Master of Science
in
Computer Science and Applications

Yang Cao, Chair
Adrian Sandu
Shu-Ming Sun

May 5, 2016
Blacksburg, Virginia

Keywords: Gillespie Algorithm, Finite Difference Method, Toxoplasma Gondii, Transmission Dynamics, Stochastic Simulation, Compartment-Based Model,

A Stochastic Model for The Transmission Dynamics of Toxoplasma Gondii

Guangyue Gao

(ABSTRACT)

Toxoplasma gondii (T. gondii) is an intracellular protozoan parasite. The parasite can infect all warm-blooded vertebrates. Up to 30% of the world's human population carry a Toxoplasma infection [30]. However, the transmission dynamics of T. gondii has not been well understood , although a lot of mathematical models have been built. In this thesis, we adopt a complex life cycle model developed by Turner et al. [34] and extend their work to include diffusion of hosts. Most of researches focus on the deterministic models. However, some scientists have reported that deterministic models sometimes are inaccurate or even inapplicable to describe reaction-diffusion systems, such as gene expression. In this case stochastic models might have qualitatively different properties than its deterministic limit. Consequently, the transmission pathways of T. gondii and potential control mechanisms are investigated by both deterministic and stochastic model by us. A stochastic algorithm due to Gillespie, based on the chemical master equation, is introduced. A compartment-based model and a Smoluchowski equation model are described to simulate the diffusion of hosts. The parameter analyses are conducted based on the reproduction number $\mathscr{R}_0$. The analyses based on the deterministic model are verified by stochastic simulation near the thresholds of the parameters.

Dedication

This thesis is dedicated to my parents.

For their endless love, support and encouragement

Acknowledgments

Firstly, I would like to express my sincere gratitude to my advisor Dr. Yang Cao for the guidance of my master study, for his patience, motivation, and immense knowledge. His guidance helped me in all the time of research and writing of this thesis.

I would also like to thank Dr. Shu-Ming Sun, Dr. Adrian Sandu for serving on my committee.

I am very thankful to my friends, my teachers and the Virginia Tech Computer Science Department for all their support. Finally, I thank my family members for their love and encouragement.

Contents

List of Figures

List of Tables

Chapter 1

Introduction

Toxoplasma gondii (T. gondii) is an obligate, single-celled, intracellular protozoan parasite, which is highly transmissible and can even alter hosts' behavior to increase their own transmission. The parasite can infect all warm-blooded vertebrates. Up to 30% of the world's human population carry a Toxoplasma infection [30]. The infection can cause life-threatening encephalitis in immunocompromised persons such as AIDS patients or recipients of organ transplants. Each year, foodborne Toxoplasmosis results in 3 billion dollars in direct medical costs and causes significant loss of quality life [6]. Healthy person's immune system usually keeps the parasite from causing illness. However, for pregnant women and individuals who have compromised immune systems, the infection could cause serious healthy problems. Furthermore, the infected people can pass the infection to their babies. The infants may not have any symptoms from the infection at birth but can develop serious symptoms later in life. The parasite can damage the infants' eyes, nervous system and ears. Occasionally, the infection may cause serious eye or brain damage at birth. Toxoplasmosis also has significant effects on human and animal behavior and may lead to neuropsychiatric disorders.

The transmission of Toxoplasma is a complex life cycle. The parasites complete their sexual reproduction in definitive hosts, meanwhile they also infect intermediate hosts in which asexual replication occurs [14]. Felids (domestic cats) have been known as the only definitive hosts in which the parasites can reproduce sexually to generate oocysts. All warm-blooded vertebrates (such as birds, mice, and sheep), can serve as intermediate hosts [33], in which asexual replication occurs. As the primary hosts of T. gondii, infected cats shed unsporulated oocysts in the environments. Within 1-5 days, oocysts in the environments sporulate and become infectious. The large number of intermediate hosts including mice get infected by ingesting these oocysts from contaminated environments. The intermediate hosts may also pass the parasites to their offsprings which is called vertical transmission. Many facts show that the susceptible cats mainly get infected by ingesting tissues of infected mice. Meanwhile cats may become infected by contacting sporulated oocysts too. However, we need to note that, comparing with consuming infected prey, cats rarely get infected by

oocysts. Dubey found that [13] cats can develop immunity to the T. gondii after primary infection. Such immunity may vanish after a period of years in the absence of continual challenge. But some researches reveal that the infected cats rarely get infected again once they are recovered. Finally, more and more evidences suggest that the cats rarely pass the parasites to their offsprings. For human, infection may remain throughout the life. Tissue cysts are most commonly found in skeletal muscle, the brain, and eyes.

A lot of mathematical models have been built to explore the transmission dynamics of T. gondii. Mateus-Pinilla et al. [29] built up the first mathematical model to describe the transmission of T. gondii. Their work investigated the transmission on swine farms with a primary focus on the importance of a feline T. gondii vaccine. They revealed that the initial T. gondii prevalence in cats has no effect on the T. gondii prevalence in finishing pigs, and that vaccination had less impact on decreasing T. gondii infection in finishing pigs than did a decrease in the number of farm cats. Arenas et al. [5] developed a mathematical model of transmission within a cat population to investigate the influence of a continuous vaccination schedule. They showed that the basic reproduction number completely determines the global dynamics and the outcome of the disease. However both of them ignored the predation-prey cycle and its impact on the transmission. Lélu et al.[26] developed the first model to investigate the complex life cycle of T. gondii transmission. In their model, The cats (definitive hosts) can become infected either via predation of infected mice (intermediate hosts) or directly from ingesting oocysts in a simple life cycle. The analysis showed that there exists a threshold for the predation rate which can determine whether the simple life cycle or the complex life cycle dominates the spread of T. gondii. Turner et al.[34] investigated the influences of various transmission pathways of T. gondii. Their model extended Lélu's work to include explicit considerations of virulence, vertical transmission, and change of host behavior, as well as vaccine and harvest controls.

However, these models are all deterministic and ignore the stochasticity that characterizes random biological behaviors. Moreover, the diffusion of hosts is missed in such models. Here, Turner's Model [34] is adopted, since it includes the most of transmission pathways of T. gondii in the complex life cycle. Furthermore, the diffusion terms are incorporated to this model by us to investigate the effects of diffusion of hosts. When we model some chemical reactions, there are only limited number of molecules involved in the reactions comparing with the large amount of total species and molecules. Consequently, the events are not enough to make average meaningful. In this case, the stochastic models provide a more detailed understanding of the reaction-diffusion processes. In this thesis, the stochastic simulations of transmission dynamics of T. gondii are given using Gillespie method. The purpose is to check whether the random biological behaviors affect the transmission dynamics by comparing with the deterministic model.

The rest of this thesis is organized as follows. The transmission model of T. gondii is presented in Chapter 2. In this Chapter, we present some basic assumptions which are used to analyze the model. The parameter values are also given. We begin Chapter 3 by formulating the chemical master equation from the theory of chemical kinetics. In this chapter, the

Stochastic Simulating Algorithm (SSA) (which is equivalent to chemical master equation) is presented. The algorithm is based on the creative work of Gillespie [21]. In Section 3.4, we focus on models of diffusion which are later used for the stochastic modeling of reaction-diffusion processes. Here, we introduce two models to simulate diffusion. One is called compartment-based model. Coupling this model with the reactions is straightforward. The second one is based on the Smoluchowski equation which is much more mathematically fundamental. We also introduce further theoretical concepts, including the Reaction-Diffusion Master Equation (RDME) and the Fokker-Planck equation. In the last Chapter, we compare the deterministic result (using finite difference scheme) with stochastic result (using SSA) to see if the stochastic model produce any qualitatively different properties? In Section 4.2, the basic reproduction number $\mathscr{R}_0$ is introduced to analyze the stability of equilibrium states of system. Basically, There are two equilibria for SIR model: one is an endemic equilibrium, and the other one is a disease free equilibrium. The threshold $\mathscr{R}_0$ allows us to determine if the model predicts parasite extinction or persistence. If $\mathscr{R}_0 < 1$, then the disease free equilibrium is locally asymptotically stable; whereas if $\mathscr{R}_0 > 1$, then it is unstable. Following Turner et. al's work [34], parameter studies are conducted to analyze the significance of vaccination rate, carrying capacity, predation rate, and behavioral change parameter. We also set up the stochastic model near the threshold values of those parameters to investigate if the stochastic results agree with the analyses based on the deterministic model. The simulation results demonstrate that the control process, including vaccination of cats and harvesting of mice can inhibit the transmission of T. gonddi. However, the level of vaccination may not be achievable in those densely populated regions. In the last section, a model including a simple end receiver, sheep, is considered. The stochastic model is also given for this more complicated model.

Chapter 2

Mathematical Model of The Transmission

In this thesis, Turner's Model [34] is adopted. They developed a deterministic SIR (susceptible-infected-recovered) model to describe the complete life cycle of parasite's transmission. The model only focuses on the transmission among cats, mice, and environments. The schematic of the transmission routes of T.gondii is given in Fig. (2.1). Generally, the environments are contaminated by excreting unsporulated oocysts of infected cats. Within one to five days after excretion, under sufficient conditions of humidity and temperature, oocysts sporulate and become infectious for hosts. The definitive hosts (cats) mainly get infected by consuming tissue cysts of infected mice. Sometimes they also become infected by ingesting oocysts in the contaminated environment. However, this rate is much lower [11]. The intermediate hosts (mice) also get infected by either of these two sources. However sporulated oocysts are more infectious for mice than for cats. Vertical transmission from mother to their offsprings occurs in all host species but only concerns susceptible females infected during pregnancy. This phenomenon rarely happens in cats, whereas it is very common in mice. Dubey [10] and Tenter [33] showed that tissue cysts persist for the whole life of the mice, whereas the infected cats can develop life-long immunity to the parasites. In this model, the transmission among mice via cannibalism is ignored.

2.1 Cats

The model splits total cat population N_c into three parts, S_c, I_c and R_c, representing the number of susceptible, infected and immune cats. In a parasite-free environment, the dynamics of the cat population is supposed to be logistic. The total population N_c of cats depends on the birth rate b_c, the mortality rate m_c, the intrinsic growth rate $r_c = b_c - m_c$ and cats carrying capacity K_c. Using Lotka-Volterra model, the dynamics is described by

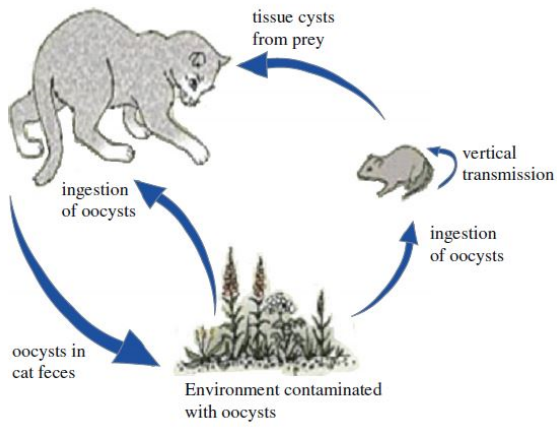

Figure 2.1: Schematic of the transmission routes of T. gondii [25].

the following differential equation:

$$\dot{N}_c = (r_c - r_c N_c/K_c)N_c = b_c N_c - (m_c + (b_c - m_c)N_c/K_c)N_c. \tag{2.1.1}$$

A lot of researches show that the immunity persists for the whole life of cats. Consequently, two assumptions are given in this model:

- recovered or vaccinated cats develop life-long immunity to the parasites,
- neither infection nor immunity is transferred from cats to their offsprings.

Cats may be infected in either of two ways. In the first transmission path, cats are infected through contact with an environments contaminated by oocysts. Denote the transmission rate by β_c, the proportion of the contaminated environments by E. The population of I_c can be described by $\beta_c E S_c$. In the second path, cats may become infected by ingesting infected mice with probability g. Here, the probability g is given by

$$g(\nu) = e^{-\frac{(\nu-0.3)^2}{2\delta^2}}, \tag{2.1.2}$$

where ν is a virulent parameter which is related to the mortality rate of mice. The maximum of ν is 0.3. T. gondii can form discrete, persistent, and genetic differentiated clonal lineages. One lineage has become especially widespread and predominant in geographically disparate locales. For modeling purpose, a trade-off may exist between parasites optimized for transmission to predators and those optimized for transmission to offsprings. Virulent factor ν is assumed to increase the infectiousness of parasite to cats. As a result, the cats are more prone to be ingested by ingestion of tissues of mice. Furthermore, the higher value of ν will shorten life and reduce offsprings of infected cats. Meanwhile, it also decreases the survivorship of mice and other intermediate hosts.

Next, we use $\theta a N_c$ to denote predation rate, where aN_c is the natural predation rate of mice and θ is the behavioral influence factor which is used to model the behavioral change of infected mice. Vyas et al. [39] showed that the parasite T.gondii will manipulate infected mice in ways that enhance parasite transmission. Specifically, the infected mice may lose their aversion to cats' odors, thereby increasing the risk to be killed by cats. Such behavioral modification would increase the possibility of parasite transmission via predation and might decrease the contribution of vertical transmission. This phenomenon is modeled by the parameter θ. Consequently, we assume that the parasite manipulates infected mice so as to alter their rate of predation αN_c by a factor θ, which satisfies:

- $\theta = 1$, the infection causes no change in the behavior of mice,
- $0 \leq \theta < 1$, the infection causes the mice to alter their behavior to avoid predation,
- $\theta > 1$, the infection increases the likelihood that the infected mice get killed by cats.

Finally, we denote cats recover rate by γ and vaccination rate by V. The complete transmission dynamics of cats discussed above is given by the following ODEs:

$$\begin{cases} \dot{S}_c = b_c N_c - \left(m_c + (b_c - m_c)\dfrac{N_c}{K_c}\right) S_c - \beta_c E S_c - g(\nu)\theta a S_c I_m - V S_c, \\ \dot{I}_c = -\left(m_c + (b_c - m_c)\dfrac{N_c}{K_c}\right) I_c + \beta_c E S_c + g(\nu)\theta a S_c I_m - \gamma I_c, \\ \dot{R}_c = -\left(m_c + (b_c - m_c)\dfrac{N_c}{K_c}\right) R_c + \gamma I_c + V S_c. \end{cases} \tag{2.1.3}$$

2.2 Mice

The evidences show that tissue cysts persist for the whole life of the mice, i.e., the infected mice develop life-long infection of parasites. According to this evidence, the model splits total mice population N_m into two parts, S_m and I_m, representing the number of susceptible and infected mice. Without outside influences, we assume that the population of mice grows logistically with intrinsic growth rate $r_m = b_m - m_m$, where b_m is the nature birth rate and m_m is the nature mortality rate. Let K_m denote the carrying capacity of mice, the transmission dynamics of mice is described by the following differential equation:

$$\dot{N_m} = (r_m - r_m N_m/K_m)N_m = b_m N_m - (m_m + (b_m - m_m)N_m/K_m)N_m. \tag{2.2.1}$$

There are two transmission routes that mice may get infected. Firstly, just as with cats, susceptible mice can get infected through ingestion of sporulated oocysts shed by cats in the contaminated environments. The transmission rate is denoted β_m. Furthermore, the infection rate of environment contamination can be described by $\beta_m E S_m$. Secondly, the

infection may come from their infected parents which we called vertical transmission. It was traditionally believed that the primary transmission route of mice was infection through contact with oocysts in the contaminated environments and subsequent asexual replication. A few papers [29, 32] have shown that the high frequency of vertical transmission may play a more significant role in the complex life cycle of T. gondii. Hide et al. [24] showed that the vertical transmission rate p_m of mice was as high as 75%. This result suggests that vertical transmission path may be more significant than previously believed. Furthermore, recent studies verified that the mortality rate of infected mice I_m is increased by virulent parameter ν. Note that in this model, the transmission among mice via cannibalism is ignored, since the transmission rate of this path is much lower than the first two routes we mentioned. Based on above discussions, the transmission dynamics of mice is thus governed by the following ODEs:

$$\dot{S}_m = b_m S_m + b_m(1-p_m)I_m - \left(m_m + (b_m - m_m)\frac{N_m}{K_m}\right) S_m, \tag{2.2.2}$$

$$\dot{I}_m = b_m p_m I_m - \left(m_m + v m_m + (b_m - m_m)\frac{N_m}{K_m}\right) I_m. \tag{2.2.3}$$

Finally, in order to control the spread of infection, let us denote harvest rate of mice by H. The complete transmission dynamics of mice is given as follows

$$\begin{cases} \dot{S}_m = b_m S_m + b_m(1-p_m)I_m - \left(m_m + (b_m - m_m)\frac{N_m}{K_m}\right) S_m - \beta_m E S_m - a N_c S_m - H S_m, \\ \dot{I}_m = b_m p_m I_m - \left(m_m + \nu m_m + (b_m - m_m)\frac{N_m}{K_m}\right) I_m + \beta_m E S_m - \theta a N_c I_m - H I_m. \end{cases} \tag{2.2.4}$$

2.3 Transmission Dynamics of Hosts and Environments

The model assumes a homogeneous use of the excreting sites by cats. The environment becomes contaminated through sporulated oocysts shed by infected cats. Oocysts survive 46-183 days in uncovered faecal deposits and 76-334 days in covered faecal deposits ([15],[33]). Clear sites are contaminated by infected cats with a rate of λ. Meanwhile, the contaminated areas decontaminate with a rate of d_0. As a result, the proportion of the contaminated environments E can be modeled by

$$\dot{E} = \lambda I_c - d_0 E. \tag{2.3.1}$$

In this model, we assume that infection does not affect the mortality and fecundity of hosts. The complete transmission dynamics of T.gondii is described by a system of ODEs

$$\begin{cases} \dot{S}_c = b_c N_c - \left(m_c + (b_c - m_c)\dfrac{N_c}{K_c}\right) S_c - \beta_c E S_c - g(\nu)\theta a S_c I_m - V S_c \\ \dot{I}_c = -\left(m_c + (b_c - m_c)\dfrac{N_c}{K_c}\right) I_c + \beta_c E S_c + g(\nu)\theta a S_c I_m - \gamma I_c \\ \dot{R}_c = -\left(m_c + (b_c - m_c)\dfrac{N_c}{K_c}\right) R_c + \gamma I_c + V S_c \\ \dot{E} = \lambda I_c - d_0 E \\ \dot{S}_m = b_m S_m + b_m(1-p_m) I_m - \left(m_m + (b_m - m_m)\dfrac{N_m}{K_m}\right) S_m - \beta_m E S_m - a N_c S_m - H S_m \\ \dot{I}_m = b_m p_m I_m - \left(m_m + \nu m_m + (b_m - m_m)\dfrac{N_m}{K_m}\right) I_m + \beta_m E S_m - \theta a N_c I_m - H I_m. \end{cases} \tag{2.3.2}$$

However, this model is deterministic and ignores the stochasticity that characterizes random biological behaviors. Moreover, it does not consider the diffusion of hosts. In this thesis, the transmission dynamics of T.gondii with diffusion of hosts is also considered by us:

$$\begin{cases} \dot{S}_c = b_c N_c - \left(m_c + (b_c - m_c)\dfrac{N_c}{K_c}\right) S_c - \beta_c E S_c - g(\nu)\theta a S_c I_m - V S_c + D_c \dfrac{\partial^2 S_c}{\partial x^2} + D_c \dfrac{\partial^2 S_c}{\partial y^2} \\ \dot{I}_c = -\left(m_c + (b_c - m_c)\dfrac{N_c}{K_c}\right) I_c + \beta_c E S_c + g(\nu)\theta a S_c I_m - \gamma I_c + D_c \dfrac{\partial^2 I_c}{\partial x^2} + D_c \dfrac{\partial^2 I_c}{\partial y^2} \\ \dot{R}_c = -\left(m_c + (b_c - m_c)\dfrac{N_c}{K_c}\right) R_c + \gamma I_c + V S_c + D_c \dfrac{\partial^2 R_c}{\partial x^2} + D_c \dfrac{\partial^2 R_c}{\partial y^2} \\ \dot{E} = \lambda I_c - d_0 E \\ \dot{S}_m = b_m S_m + b_m(1-p_m) I_m - \left(m_m + (b_m - m_m)\dfrac{N_m}{K_m}\right) S_m - \beta_m E S_m \\ \qquad - a N_c S_m - H S_m + D_m \dfrac{\partial^2 S_m}{\partial x^2} + D_m \dfrac{\partial^2 S_m}{\partial y^2} \\ \dot{I}_m = b_m p_m I_m - \left(m_m + \nu m_m + (b_m - m_m)\dfrac{N_m}{K_m}\right) I_m + \beta_m E S_m \\ \qquad - \theta a N_c I_m - H I_m + D_m \dfrac{\partial^2 I_m}{\partial x^2} + D_m \dfrac{\partial^2 I_m}{\partial y^2}. \end{cases} \tag{2.3.3}$$

The diffusion of hosts is modeled by Fokker-Planck equation, where D_c and D_m are diffusion rates of cats and mice respectively. In this model, We consider a 1 km^2 square farm which is divided into 10×10 cells. To track the positions of the hosts as well as the distribution of oocycsts, we assign a unique coordinate for each cell. Assume that the daily activities of a cat occur in a square of 6×6 cells and the daily activities of a mouse occur in a square of 1.2×1.2 cells. The daily changes of positions of the hosts are governed by the random walk

Variable	Refer to	Value
b_c	Cats Birth Rate	2.4/52
m_c	Cats Death Rate	0.6/52
r_c	$r_c = b_c - m_c$	1.8/52
β_c	Environment Transmission Rate to Cats	0.54/52
γ	Cats Recovery Rate	0.5
K_c	Cats Carrying Capacity	50
V	Cats Vaccination Rate	0.7
α	Cats Predation Rate	2e-5

Table 2.1: Parameters of Cats.

rule. We also assume that no flux on the boundaries, which means the farm is an enclosed area. Therefore, we can assign the following Neumann conditions $\partial_n S_c = 0$, $\partial_n I_c = 0$, $\partial_n R_c = 0$, $\partial_n S_m = 0$ and $\partial_n I_m = 0$ to each boundary.

2.4 Parameters

In this thesis, both deterministic model and stochastic model are simulated by us. The parameters are obtained from the available literature [26]. The exact values and explanations are given in Table (2.1), Table (2.2), and Table (4.2). For cats, b_c and m_c were already used in modeling the spread of feline viruses [8]. For mice, m_m and b_m are chosen in accordance with the fecundity and mortality observed in [27]. The contamination rate of environment λ is estimated by Afonso et al. [1] through a 15 weeks survey. The decontamination rate of environment is given by Dumetre [15]. β_c and β_m are estimated from results of Afonso et al. ([1], [2], and [3]), which deal with the transmission of T. gondii in the sparsely populated regions.

Variable	Refer to	Value
b_m	Mice Birth Rate	6/52
m_m	Mice Death Rate	2/52
r_m	$r_m = b_m - m_m$	4/52
β_m	Environment Transmission Rate to Mice	0.6767
K_m	Mice Carrying Capacity	300
p_m	Vertical Transmission Probability	0.75
θ	Mice Behavioral change rate	1.2
H	Harvesting Rate of Mice	1/52

Table 2.2: Parameters of Mice.

Chapter 3

Stochastic Simulation

3.1 Introduction

There are two fundamental approaches to the mathematical models of chemical reactions and diffusion: one is deterministic model and the other one is stochastic model. The deterministic models are mainly based on differential equations, in which the output of the model is fully determined by the parameter values and the initial conditions. However, when we model some chemical reactions, there are only limited number of molecules involved in the reactions, comparing with the large amount of total species and molecules. As a consequence, there are not enough events to make average meaningful which makes deterministic models cannot describe the process accurately. This problem also arises in some other mathematical models comprising essentially discrete events, such as stock trading and gene regulation. On the other hand, in biological system, the fluctuations (e.g. switching between two favorable states of the system) have a profound effects on the dynamics of the system and may determine the final outcome. Importantly, these fluctuations prohibit the use of deterministic method to model the system. Van Kampen [37] showed that the number of fluctuations of random reaction in a system of m molecules will be of the order $m^{-1/2}$. In another word,

$$\text{Fluctuations of random interactions} = \frac{\text{random component}}{\text{deterministic component}} = \frac{1}{\sqrt{m}}.$$

If this ratio is significant we cannot use the deterministic model to describe the process. In this case, the stochastic model may provide a more detailed understanding of the reaction-diffusion process. Recently, the role of stochastic simulation has been more and more popular in biological process, such as pattern formation, cell division, and morphogenesis.

3.2 Chemical Kinetics and The Master Equation

Generally, the stochastic dynamics of a spatially homogeneous system is governed by the reaction master equation (RME) [19, 21]. Gillespie [21] mentioned that the probabilistic model for chemical reactions can be developed by a set of random movements. The chemical reactions usually occur only if two molecules are close enough, i.e., the distance between their centers are shorter than the sum of their radii. If we assume that the system is in thermal equilibrium so that the molecules are uniformly distributed, they will collide with each other at random. Some experiences even show that the reactions occur only if special areas on the surface called "binding sites" of the molecules collide. Consequently, we may assign a certain probability to the event that molecules react upon collision. For example, considering a simple reaction,

$$A + B \xrightarrow{k_1} C, \tag{3.2.1}$$

where A and B are two reactants. Given that there is a certain probability of A and B will collide and react, we may assume that the likelihood of reaction (3.2.1) occurring is proportional to the number of combinations of reactant molecules A and B. Furthermore, assume that k_1 is the constant rate of proportionality. Following these assumptions, we can introduce the important concept of chemical reactions, the propensity function. In our case, let $\mathbf{v}_1 = [A(t), B(t)]$ be a state vector used to denote the number of molecules of A and B at time t. the propensity function of (3.2.1), $\alpha(\mathbf{v}_1)$ is defined by

$$\alpha(\mathbf{v}_1) = k_1 A(t) B(t).$$

Obviously, the propensity function is determined by the copy numbers of reactants A and B, as well as the rate constant k_1. Given that the system was at state $\mathbf{v}_1$ at time t, the propensity function $\alpha(\mathbf{v}_1)$ is defined such that $\alpha(\mathbf{v}_1)dt$ is the probability that reaction (3.2.1) will occur in the time interval $[t, t + dt)$.

In this model, we consider a system with 6 species $[S_c, I_c, R_c, S_m, I_m, E]$. The numbers of them at time t are denoted by $[S_c(t), I_c(t), R_c(t), S_m(t), I_m(t), E(t)]$. Mathematically, the time evolutions of these species are calculated by solving the system of coupled ordinary differential equations given in chapter 2. Each equation expresses the time-rate-of-change of the concentration of one species as a function of the concentrations of all the species. This traditional method of analysis is based on a deterministic formulation of chemical kinetics. In the deterministic formulation, the reaction constants are viewed as reaction rates and the species concentrations are represented by continuous functions of time t. A more broadly applicable approach to the chemical kinetics is the stochastic formulation. Here the reaction constants are viewed as reaction probabilities per unit time. Before we do the stochastic simulation, the deterministic model (2.3.3) should be converted into stochastic formulations. (The details can be found in [21]). In our model, a list of the stochastic formulations and their associated propensity functions can be found in Table (3.1) and Table (3.2). We need to note that the parameters given in chapter 2 are all about concentrations of species. However the stochastic formulations are all related to the population of species. In conversion, especially

Transition	Reaction	Propensity	Affects	Depends
S_c generation	$S_c \xrightarrow{b_c} 2S_c$	$\alpha_1 = b_c S_c$	S_c	S_c
I_c generation	$I_c \xrightarrow{b_c} S_c + I_c$	$\alpha_2 = b_c I_c$	S_c, I_c	I_c
S_c degradation	$S_c \xrightarrow{m_c + r_c \frac{N_c}{K_c}} \emptyset$	$\alpha_3 = \left(m_c + r_c \frac{N_c}{K_c}\right) S_c$	S_c	S_c
S_c to I_c by E	$S_c \xrightarrow{\beta_c E} I_c$	$\alpha_4 = \beta_c E S_c$	S_c, I_c	S_c
S_c to I_c by I_m	$S_c + I_m \xrightarrow{g\theta a} I_c$	$\alpha_5 = g\theta a S_c I_m N^2$	S_c, I_m, I_c	S_c, I_m
S_c to R_c by Vaccination	$S_c \xrightarrow{V} R_c$	$\alpha_6 = V S_c$	S_c, R_c	S_c
I_c degradation	$I_c \xrightarrow{m_c + r_c \frac{N_c}{K_c}} \emptyset$	$\alpha_7 = \left(m_c + r_c \frac{N_c}{K_c}\right) I_c$	I_c	I_c
I_c to R_c by recover	$I_c \xrightarrow{\gamma} R_c$	$\alpha_8 = \gamma I_c$	I_c, R_c	I_c
R_c degradation	$R_c \xrightarrow{m_c + r_c \frac{N_c}{K_c}} \emptyset$	$\alpha_9 = \left(m_c + r_c \frac{N_c}{K_c}\right) R_c$	R_c	R_c

Table 3.1: Stochastic Formulations and Propensity Functions of Cats.

for those reactions with two reactants, we need to do some transformation such that the deterministic model is consistent with stochastic model. For example, in our case, we divide 1 km^2 farm into $N * N$ squares. For each square, the area should be $1/N^2 km^2$. Considering the reaction 5, the original deterministic formulation is given by

$$\frac{d[I_c]}{dt} = g\theta\alpha[S_c][I_m],$$

where $[I_c], [S_c]$, and $[I_m]$ are concentrations of corresponding species. When we do the conversion, we need to convert them into population by multiplying the area on both sides

$$\begin{aligned} \frac{1}{N^2}\frac{dI_c}{dt} &= g\theta\alpha[S_c]I_m\frac{1}{N^2} \\ \frac{dI_c}{dt} &= N^2 g\theta\alpha S_c I_m. \end{aligned}$$

Therefore the propensity function α_5 is $N^2 g\theta\alpha S_c I_m$ rather than $g\theta\alpha S_c I_m$.

In the stochastic formulation of chemical kinetics, the time evolution is not determined by a set of coupled differential equations related to the species concentrations, but rather by a single differential-difference equation for a grand probability function in which time and the species population all appear as independent variables. This differential-difference equation is called the master equation. In order to make the further discussion easier, let us introduce some notations which will be used later. Firstly, let R denote a reaction. In our system, $19th$ reactions are denoted by R_i for $1 \leq i \leq 19$. When the reaction R_i occurs, all reactants related to this reaction may alter their copy numbers. Thus we let $\mathbf{c}_i$ be the vector of coefficients that adjusts the copy numbers of each species in the system according to the

Transition	Reaction	Propensity
S_m generation from S_m	$S_m \xrightarrow{b_m} 2S_m$	$\alpha_{10} = b_m S_m$
S_m generation from I_m	$I_m \xrightarrow{b_m(1-p_m)} I_m + S_m$	$\alpha_{11} = (b_m(1-p_m))\, I_m$
S_m degradation	$S_m \xrightarrow{m_m + r_m \frac{N_m}{K_m}} \emptyset$	$\alpha_{12} = \left(m_m + r_m \frac{N_m}{K_m}\right) S_m$
S_m degradation by cats	$S_m \xrightarrow{\alpha N_c} \emptyset$	$\alpha_{13} = \alpha N_c S_m N^2$
S_m degradation by Harvest	$S_m \xrightarrow{H} \emptyset$	$\alpha_{14} = H S_m$
S_m to I_m by E	$S_m \xrightarrow{\beta_m E} I_m$	$\alpha_{15} = \beta_m E S_m$
I_m generation	$I_m \xrightarrow{b_m p_m} 2I_m$	$\alpha_{16} = b_m p_m I_m$
I_m degradation	$I_m \xrightarrow{(1+\nu)m_m + r_m \frac{N_m}{K_m}} \emptyset$	$\alpha_{17} = \left((1+\nu)m_m + r_m \frac{N_m}{K_m}\right) I_m$
I_m degradation by Cats	$I_m \xrightarrow{\theta \alpha N_c} \emptyset$	$\alpha_{18} = \theta \alpha N_c I_m N^2$
I_m degradation by Harvest	$I_m \xrightarrow{H} \emptyset$	$\alpha_{19} = H I_m$

Table 3.2: Stochastic Formulations and Propensity Functions of Mice.

reaction R_i. For example, considering reaction 5 in the Table (3.1), the vector c_5 is given as follows:

$$\mathbf{c}_5 = [\Delta S_c, \Delta I_c, \Delta R_c, \Delta S_m, \Delta I_m, \Delta E] = [-1, +1, 0, 0, -1, 0].$$

Note that the species E is actually a proportion. We will discuss how to convert the differential equation containing E into stochastic formulations in Chapter 4. In the rest of this chapter, only 5 species are considered. Finally we denote by $P(\mathbf{v}, t|\mathbf{v}_0, t_0)$ the conditional probability that the system is in state v at time t given that it was in state v_0 at time t_0. To introduce the chemical master equation, without loss of generality, assume we have M reactions R_i, $1 \le i \le M$. Considering the time interval $[t, t+dt)$, suppose that at most one reaction occurs during dt. The probability that no reaction occurs in $[t, t+dt)$ is given by

$$P(\mathbf{v}, t|\mathbf{v}_0, t_0) P(\text{no change over } dt) = P(\mathbf{v}, t|\mathbf{v}_0, t_0) \left[1 - \sum_{i=1}^{M} \alpha_i(\mathbf{v}) dt\right],$$

and the probability that reaction R_i occurs during dt is given by $P(\mathbf{v}-\mathbf{c}_i, t|\mathbf{v}_0, t_0)\alpha_i(\mathbf{v}-\mathbf{c}_i)dt$. Since they are mutually exclusive, we may combine them additively. Therefore

$$\begin{aligned} P(\mathbf{v}, t+dt|\mathbf{v}_0, t_0) &= P(\mathbf{v}, t|\mathbf{v}_0, t_0) P(\text{no change over } dt) \\ &\quad + \sum_{i=1}^{M} P(\mathbf{v}-\mathbf{c}_i, t|\mathbf{v}_0, t_0) P(\text{state change over } dt) \\ &= P(\mathbf{v}, t|\mathbf{v}_0, t_0) \left[1 - \sum_{i=1}^{M} \alpha_i(\mathbf{v}) dt\right] \\ &\quad + \sum_{i=1}^{M} P(\mathbf{v}-\mathbf{c}_i, t|\mathbf{v}_0, t_0) \alpha_i(\mathbf{v}-\mathbf{c}_i) dt. \end{aligned}$$

Subtracting $P(\mathbf{v}, t|\mathbf{v}_0, t_0)$ from both sides and dividing by dt, we then obtain

$$\frac{P(\mathbf{v}, t+dt|\mathbf{v}_0, t_0) - P(\mathbf{v}, t|\mathbf{v}_0, t_0)}{dt} = \sum_{i=1}^{M} \left[\alpha_i(\mathbf{v}-\mathbf{c}_i)P(\mathbf{v}-\mathbf{c}_i, t|\mathbf{v}_0, t_0) - \alpha_i(\mathbf{v})P(\mathbf{v}, t|\mathbf{v}_0, t_0)\right].$$

As a shorthand we use $P(\mathbf{v})$ to substitute $P(\mathbf{v}, t|\mathbf{v}_0, t_0)$, then we obtain

$$\frac{\partial P(\mathbf{v})}{\partial t} = \sum_{i=1}^{M} \left[\alpha_i(\mathbf{v}-\mathbf{c}_i)P(\mathbf{v}-\mathbf{c}_i) - \alpha_i(\mathbf{v})P(\mathbf{v})\right], \tag{3.2.2}$$

which is called master equation. As what we mentioned, the master equation is a differential-difference equation depending on probability function. Specifically, in our case, the master equation without considering diffusion is given as follows:

$$\begin{aligned}
\frac{\partial P(S_c, I_c, R_c, S_m, I_m)}{\partial t} &= N_c b_c P(S_c - 1, I_c, R_c, S_m, I_m) - N_c b_c (S_c, I_c, R_c, S_m, I_m) \\
&+ \left(m_c + r_c \frac{N_c}{K_c}\right)(S_c + 1)P(S_c + 1, I_c, R_c, S_m, I_m) \\
&- \left(m_c + r_c \frac{N_c}{K_c}\right) S_c P(S_c, I_c, R_c, S_m, I_m) \\
&+ \beta_c E(S_c - 1)P(S_c + 1, I_c - 1, R_c, S_m, I_m) \\
&- \beta_c E S_c P(S_c, I_c, R_c, S_m, I_m) \\
&+ \ldots
\end{aligned}$$

To get analytic solution of this equation is difficult. So we turn our efforts to the numerical simulation of this master equation. Actually, the simulation algorithm is fully equivalent to the master equation, even though the master equation itself is never explicitly used.

3.3 The Gillespie Algorithm

The evolution trajectory can be exactly formulated by the master equation. However, most of master equations cannot be solved analytically and therefore are of little practical use. In our case, 19 reactions are included (2 more will be introduced later)and some of them are non-linear. Even writing down the master equation would be a problem.
Gillespie[22] developed a stochastic algorithm to simulate a particular evolution of a system instead of trying to solve for all possible trajectories by the master equation. Repeated execution of the exact algorithm will give an average that corresponds to the solution of master equation.

The basic idea of this computational procedure is to use Monte Carlo techniques to simulate the stochastic process described by propensity function. The simulation algorithm

is straightforward. Set the time variable $t = 0$. Suppose that we have a system including N different chemical species denoted by S_j, $j = 1, ..., N$, which are subject to the reactions R_i, $i = 1, ..., M$. At each time step, we first ask when will the next reaction occur? The derivation is straightforward and given in [17]. Let us consider the single chemical reaction

$$A \xrightarrow{k} \emptyset, \tag{3.3.1}$$

where A is the chemical species of interest and k is the rate constant of the reaction. The symbol $\emptyset$ denotes chemical species which are of no further interest in what follows. The rate constant k is defined so that kdt gives the probability that a randomly chosen molecule of chemical species A reacts during the time interval $[t, t + d\tau)$. In particular, the propensity function that exactly one reaction (3.3.1) occurs during the infinitesimal time interval $[t, t + d\tau)$ is equal to $A(t)k$, where the number of molecules of chemical species A at time t is simply denoted by $A(t)$. Our goal is to find τ such that $t + \tau$ is the time when the next reaction (3.3.1) occurs. Suppose that there are $A(t)$ molecules at time t in the system. Let us denote by $P(A(t), s)ds$ the probability that the next reaction occurs during the time interval $[t + s, t + s + ds)$ where ds is an infinitesimally small time step. Let $h(A(t), s)$ be the probability that no reaction occurs in the interval $[t, t + s)$. Then the probability $P(A(t), s)ds$ is equal to the product of $h(A(t), s)$ and $A(t + s)kds$ which is the probability that the reaction (3.3.1) occurs in the time interval $[t + s, t + s + ds)$. Since no reaction occurs in $[t, t + s)$, we have $A(t + s) = A(t)$ which implies that

$$P(A(t), s)ds = h(A(t), s)A(t)kds. \tag{3.3.2}$$

The probability that no reaction occurs in the interval $[t, t + \sigma + d\sigma)$ can be computed as follows

$$h(A(t), \sigma + d\sigma) = h(A(t), \sigma)[1 - A(t + \sigma)kd\sigma],$$

where $1 - A(t+\sigma)kd\sigma$ means no reaction occurs in the interval $[t+\sigma, t+\sigma+d\sigma)$. Similarly, since $A(t + \sigma) = A(t)$, we may obtain that

$$\frac{dh(A(t), \sigma)}{d\sigma} = \lim_{d\sigma \to 0} \frac{h(A(t), \sigma + d\sigma) - h(A(t), \sigma)}{d\sigma} = -A(t)kh(A(t), \sigma). \tag{3.3.3}$$

With initial condition $h(A(t), 0) = 1$, the solution of ordinary differential equation (3.3.3) is given by

$$h(A(t), \sigma) = exp[-A(t)k\sigma]. \tag{3.3.4}$$

Substitute (3.3.4) into (3.3.2), we obtain

$$P(A(t), s)ds = exp[-A(t)ks]A(t)kds. \tag{3.3.5}$$

More generally, if we have M reactions, the probability that any reaction occurs in the time interval $[t + s, t + s + ds)$ is given by

$$P(A(t), s)ds = exp[-\alpha_0 s]\alpha_0 ds, \tag{3.3.6}$$

where α_0 is the sum of the individual propensities

$$\alpha_0 = \sum_{k=1}^{M} \alpha_k. \tag{3.3.7}$$

Suppose that $\tau \in (0, \infty)$ is the random number such that $t + \tau$ is the time that the next reaction occurs. It is a random number distributed according to (3.3.6). Consequently, we consider the function $F(\cdot)$ defined by

$$F(\tau) = exp[-\alpha_0 \tau]. \tag{3.3.8}$$

Since α_0 is always non-negative, the function $F(\tau)$ is monotone decreasing in the interval $(0, 1)$. Note that

$$\frac{dF(\tau)}{d\tau} = -\alpha_0 \tau exp[-\alpha_0 \tau].$$

Let a, b be two arbitrary numbers in the interval $(0, 1)$. The probability that $\tau \in (F^{-1}(b), F^{-1}(a))$ is given by the integral of $P(A(t), s)$ over s in the interval $(F^{-1}(b), F^{-1}(a))$, which is

$$\begin{aligned} \int_{F_{-1}(b)}^{F_{-1}(a)} P(A(t), s) ds &= \int_{F_{-1}(b)}^{F_{-1}(a)} exp[-\alpha_0 s] \alpha_0 ds \\ &= -\int_{F_{-1}(b)}^{F_{-1}(a)} \frac{dF(\tau)}{d\tau} ds \\ &= b - a. \end{aligned}$$

Consequently, the probability that $F(\tau) \in (a, b)$ is as same as $b - a$. Then $F(\tau)$ is a random number uniformly distributed in $(0, 1)$. Hence, in order to find τ, we can generate a uniformly distributed random number r_1 for $F(\tau)$. Using (3.3.8), we set

$$r_1 = exp[-\alpha_0 \tau].$$

Solving for τ, then the time until the next occurrence of a reaction is

$$\tau = \frac{1}{\alpha_0} \ln \left[\frac{1}{r_1} \right]. \tag{3.3.9}$$

Next, we ask that which reaction is it? Since the reactions partition the interval $(0, 1)$ according to the size of their propensity function, given a second random number r_2 uniformly distributed in $(0, 1)$, we can decide which reaction has occurred at $t + \tau$ by deciding in which partition r_2 lies. So the reaction R_μ occurs at the time $t + \tau$ can be located by

$$r_2 \geq \frac{1}{\alpha_0} \sum_{k=1}^{\mu-1} \alpha_k \quad \text{and} \quad r_2 < \frac{1}{\alpha_0} \sum_{k=1}^{\mu} \alpha_k. \tag{3.3.10}$$

The schematic can be found in (3.1).

Then the Gillespie SSA consists of the following steps:

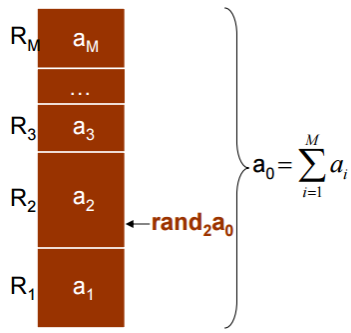

Figure 3.1: Which reaction occurs next?

1. Initialization: set the initial molecule copy numbers, set time $t = 0$.
2. Calculate the propensity function α_i for each reaction, and the total propensity according to
$$\alpha_0 = \sum_{k=1}^{M} \alpha_k.$$
3. Generate two uniformly distributed random numbers r_1 and r_2 from the range $(0, 1)$.
4. Compute the time when the next chemical reaction takes place as $t + \tau$ where τ is given by (3.3.9).
5. Decide which reaction R_μ occurs at the new time. Find μ by inequalities (3.3.10).
6. Update the state vector $\mathbf{v}$ by adding the update vector $\mathbf{c}_\mu$:
$$\mathbf{v}(t + \tau) = \mathbf{v}(t) + \mathbf{c}_\mu$$
7. Set $t = t + \tau$. Return to step 2 until t reaches some specified limit t_{MAX}.

The Gillespie algorithm provides an exact method for the stochastic simulation of systems of chemical reactions. Each execution of the Gillespie algorithm will produce a calculation of the evolution of the system. If one considers systems of many chemical reactions and many chemical species, to gather any useful information from the algorithm, it should be run many times in order to calculate a stochastic mean and variance that tells us about the behavior of the system. In such a case, even the Gillespie algorithm is an useful tool, it suffers from the drawback that as the computational time increases with the number of reactions. There are ways to make the Gillespie algorithm more efficient. In this thesis, we simulate one reaction per one time step. Thus, it makes sense to update only those propensity functions which are changed by the chemical reaction selected in step 5. As a consequence, we don't need to

waste time to recompute all the propensity functions at each time step. Gibson and Bruck introduce a more efficient computer implementation of the Gillespie algorithm. A more detail discussion can be found in their paper [20]. In summary, the Gillespie algorithm does not try to numerically solve the master equation for a given system. Actually, it numerically simulates the Markov process that the master equation describes analytically.

3.4 Stochastic Modeling of Reaction-Diffusion System

Einstein [16, 31] has shown that the small particles in a fluid possess kinetic energy which is proportional to the absolute temperature [7]. This thermal energy can make them travel in uncorrelated directions according to a velocity distribution. Diffusion is the random migration of small particles arising from this kind of motion. If we take consideration of diffusion of hosts, our model is changed to a reaction-diffusion system. In recent years, stochastic simulation of reaction-diffusion systems has drawn more and more attention in the spatially inhomogeneous biological systems, such as pattern formation. Theoretically, the stochastic dynamics of a spatially inhomogeneous system is governed by the reaction-diffusion master equation (RDME)[19]. But the RDME is computationally impossible to solve for almost all practical problems. Stochastic methods were then proposed to solve for evolution trajectories for the reaction-diffusion systems. Spatial stochastic simulation is an extremely computationally intensive task, due to the large problem dimension resulted from the discretization of the system. The most widely used stochastic method is Gillespie's Stochastic Simulation Algorithm (SSA) which we have discussed in the last section. The SSA is originally developed for well-stirre biochemical systems. The adaption of SSA to the spatial model is straightforward. In the spatial inhomogeneous model, spatial domain is discretized into small grids, where in each grid the reactants are considered well-stirred. Chemical reaction fire among species molecules in the same well-stirred grid and the diffusion is modeled as the random walk across neighboring grids. The stochastic simulation strategies on reaction-diffusion system can be categorized into two theoretical frameworks: the spatially and temporally continuous Smoluchowski modeling [38] and the compartment-based modeling, formulated as the spatially discretized reaction-diffusion master equation (RDME) [19, 21].

3.4.1 Compartment-based Model

The compartment-based modeling, formulated as the spatially discretized reaction-diffusion master equation (RDME), discretized the spatial domain for an inhomogeneous system into small grids. The reaction-diffusion master equation is coarse-grained and better suited for large scale simulations. In RDME, the spatial domain is discretized into small compartments. Within each compartment, molecules are considered well-stirred. Under RDME scheme, the diffusion is modeled as the continuous time random walk on the mesh grids, while the reactions fire only among the molecules in the same compartment. For simplicity, suppose

that we have a one dimensional (1D) domain $[0, 1]$ which is partitioned into K grids G_k, $k = 1, 2, ..., K$, each with length $h = 1/K$. Assume that N species $\{S_1, S_2, ..., S_N\}$ and M reactions $\{R_1, R_2, ..., R_M\}$ are considered. Each species population, as well as the reactions in the system will have a local copy for each grid at a given time. The state of the reaction-diffusion system at any time t is represented by the vector state

$$V(t) = \{V_{1,1}(t), V_{1,2}(t), ..., V_{1,K}(t), ..., V_{n,1}(t), ..., V_{N,K}(t)\},$$

where $V_{n,k}(t)$ represents the number of species S_n in the grid G_k at time t. We assume that the molecules are well-stirred within compartments, but not necessarily well-stirred between compartments. Reactions occur among species molecules within the same compartment, while diffusion is modeled as the Brownian motion between neighboring compartment. Molecules jump from one compartment to another. This jump can be considered as a chemical reaction. These reactions can be chained together to form a series of reactions that simulate molecules diffusing throughout the domain. For species S_1, the diffusion can be represented as follows:

$$S_{1,1} \underset{d}{\overset{d}{\rightleftharpoons}} S_{1,2} \underset{d}{\overset{d}{\rightleftharpoons}} S_{1,3} \underset{d}{\overset{d}{\rightleftharpoons}} S_{1,4} \cdots \underset{d}{\overset{d}{\rightleftharpoons}} S_{1,K}, \tag{3.4.1}$$

where $S_{1,k}$ represents the number of species S_1 in the kth grid. The rate constant d is called diffusion coefficient which is the only parameter that needs to be matched to the physical scenario. Let D denote a diffusion constant which depends on the size of the molecule. In another word, diffusive spreading will be characterized by D. Without loss of generality, we consider a 1D domain. Let $[S_1(x, t)]$ represent the concentration of S_1, which we suppose to be continuous, at a point x in the domain at time t. It can be shown that $[S_1(x, t)]$ evolves according to the partial differential equation

$$\frac{\partial[S_1(x,t)]}{\partial t} = D\frac{\partial^2[S_1(x,t)]}{\partial x^2}, \tag{3.4.2}$$

which is a special form of the so-called Fokker-Planck equation. Assume that no chemical interaction between species in the solution and the boundary of the domain. We choose to implement zero Neumann condition on each boundary, which is so-called reflective boundary condition or zero flux boundary condition. If we set

$$d = \frac{D}{h^2}, \tag{3.4.3}$$

where h is the compartment length, R. Erban et al. [17] have shown that the stochastic mean for the chain of reactions (3.4.1) will be equivalent to a discretisation of the diffusion equation (3.4.2) with Neumann boundary conditions

$$\frac{\partial[S_1(x,t)]}{\partial x}(0) = \frac{\partial[S_1(x,t)]}{\partial x}(1) = 0,$$

regardless of dimension. Moreover, we can extend this model to 2D by dividing the domain into squares, and allowing the species molecules to jump into any of the adjacent four

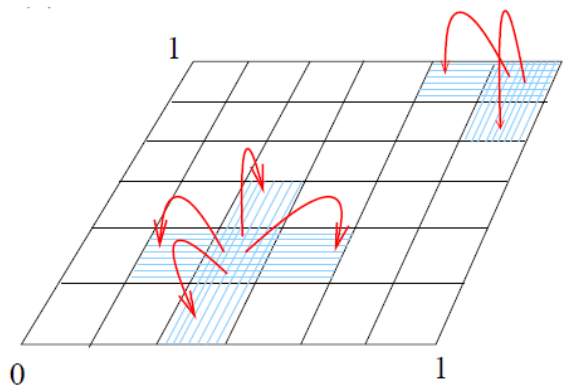

Figure 3.2: Schematic of 2D compartment based diffusion model [35].

compartment (Fig (3.4.4)). When it does so, the propensity function of all reactions in the involving compartments need to be updated.

The other benefit of the compartment-based model is that we can add chemical reactions in the model easily. The dynamics of the chemical reactions in each grid follows the same principles as chemical master equation (CME). Assume that each reaction R_j in any grid k is characterized using the propensity function $a_{j,k}$ and the state change vector $\mathbf{c}_j \equiv (\mathbf{c}_{1j}, \mathbf{c}_{2j}, ..., \mathbf{c}_{Nj},)$. The diffusion between grid G_j and G_k is characterized by the diffusion propensity function $d_{i,k,j}$ and the state change vector $\mu_{k,j}$ similarly. $d_{i,k,j}(x)dt$ gives the probability that, given $V_{i,k}(t) = x$, one molecule of species S_i at grid G_k diffuses into grid G_j in the next infinitesimal time interval $[t, t + dt)$. For the diffusion of S_1 jump from grid G_j to G_k, the state vector

$$\mu_{k,j} = \{0, 0, ..., \underbrace{-1}_{j}, ... \underbrace{1}_{k}, ...0\}.$$

Thus, the RDME for our one dimensional system can be described by:

$$\begin{aligned}
&\frac{\partial P(x,t|x_0,t_0)}{\partial t} \\
= &\sum_{k=1}^{K}\sum_{j=1}^{M}\left(a_{j,k}(x-\mathbf{c}_{j,k})P(x-\mathbf{c}_{j,k},t|x_0,t_0) - a_{j,k}(x)P(x,t|x_0,t_0)\right) \\
+ &\sum_{i=1}^{K}\sum_{k=1}^{K}\sum_{j=1}^{M}\left(-d_{i,j,k}(x_{ik})P(x,t|x_0,t_0) + d_{i,k,j}(V_{ik}-\mu_{k,j})P(V_{11},...,V_{ik}-\mu_{k,j},...,t|x_0,t_0)\right),
\end{aligned}$$

where $P(x, t|x_0, t_0)$ denotes the probability that the system state $V(t) = x$ given that $V(t_0) = v_0$.

The RDME is a set of ODEs that gives one equation for every possible states. It is both theoretically and computationally intractable to solve RDME for practical biochemical

systems due to the huge number of possible combinations of states. Instead of solving RDME for the time evolution of the probabilities, we can construct numerical realizations of $V(t)$. With enough trajectory realizations, we can derive the probabilities of each state vector at different time. Consequently, we can apply Gillespie's stochastic simulation algorithm introduced in section 3.3 to simulate each diffusive jumping and chemical reaction event explicitly.

3.4.2 Smoluchowski Equation Model

The Smoluchowski framework resolves the exact position of molecules and is mathematically more fundamental. In the Smoluchowski framework, molecules are modeled as points that diffuse as Brownian particles. Bimolecular reaction fires instantaneously, or with a fixed propensity density when two molecules fall into a certain distance, which is usually referred to as the "reaction radius".

This framework is based on the approach of von Smoluchowski. We calculate the trajectory of each molecule individually by stochastically calculating the component of the position of the molecule in each dimension. In two dimensional (2D) domain, let $[X(t), Y(t)]$ be the position of a diffusing molecule at time t. Suppose that the molecule follows a Brownian motion with its positions. Therefore the change of coordinate $X(t+\triangle t)$ is normally distributed with mean 0 and variance $2D \triangle t$. We may generate two random numbers ξ_x and ξ_y which are normally distributed with zero mean and unit variance such that the position of the diffusing molecule at time $t+\triangle t$ is given by

$$X(t+\triangle t) = X(t) + \sqrt{2D \triangle t}\xi_x, \tag{3.4.4}$$

$$Y(t+\triangle t) = Y(t) + \sqrt{2D \triangle t}\xi_y. \tag{3.4.5}$$

Note that the x-coordinate and y-coordinate are independent to each other. In Fig (3.3), assume the initial position is $(0, 0)$, two trajectories are calculated based on (3.4.4) and (3.4.5). The drawback of this method is that it is difficult to include bimolecular reactions in the model. For any two molecules, it is necessary to determine that how close they are such that the collision occurs. Furthermore, it is also necessary to decide the probability of a reaction occurring once a collision has occurred. This method becomes computationally expensive as the number of molecules grows. The reaction-diffusion SSA based on the Smoluchowski equation is nontrivial. The details can be found in [4]. Here, we choose to use compartment-based approach to simulate our model.

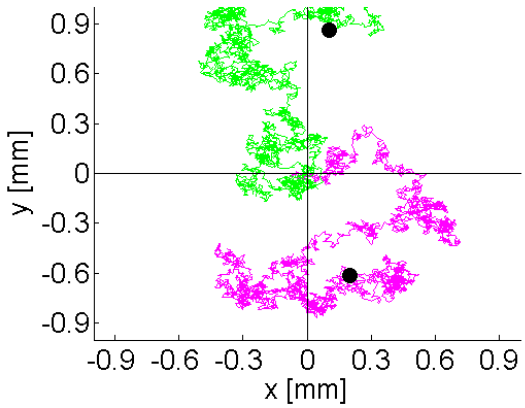

Figure 3.3: The trajectories of two molecules obtained by Smoluchowski framework.

Chapter 4

Results and Conclusion

4.1 The Comparison between Deterministic Results and Stochastic Results

We have introduced stochastic simulation algorithms for chemical reactions, molecular diffusion and reaction-diffusion processes in the previous chapter. In this chapter, we will apply compartment-based framework to simulate the stochastic model of T. gondii transmission given in the second chapter. For the simulation purpose, we consider a sparsely populated region with a carrying capacity of 50 cats and 300 mice. At beginning, we consider the deterministic model governed by ODEs (2.3.2) without diffusion terms. In this model, the vaccination of cats and harvesting of mice are introduced. Using a finite difference scheme, we obtain the numerical simulation of (2.3.2). Fig. (4.1) shows the time evolution trajectories of this model. The red line represents the results under the implementation of control. The blue line shows the case in the absence of any control. In the control case, we choose $V = 0.7$ and $H = 1/52$. The initial values of cats and mice are given in Table (4.1). We assume that 20 percent of farm is contaminated initially. All other parameters take the default values in Table (2.1), (2.2), and (4.2).

Variable	Refer to	Initial Value
S_c	Number of Susceptible Cats	6
I_c	Number of Infected Cats	1
R_c	Number of Immune Cats	0
S_m	Number of Susceptible Mice	100
I_m	Number of Infected Mice	0

Table 4.1: Initial Values of Simulation.

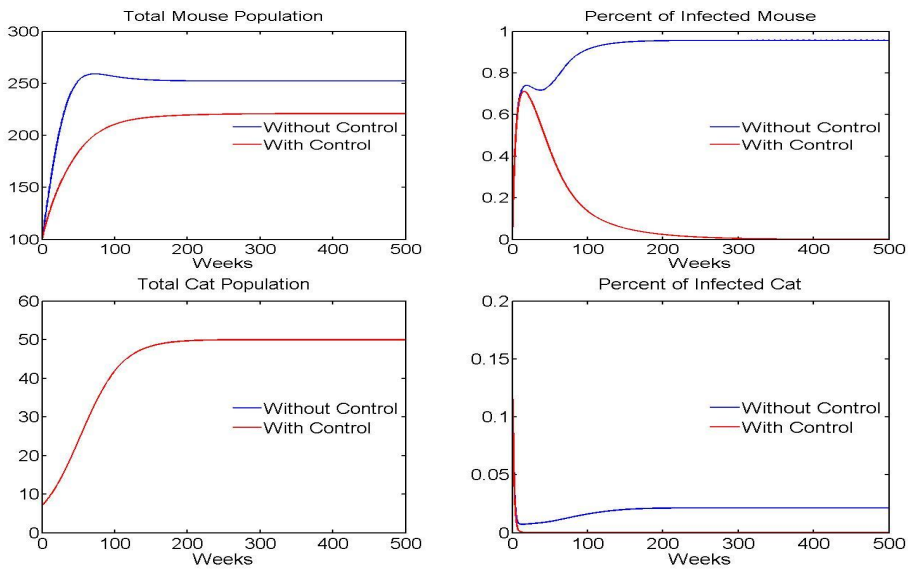

Figure 4.1: Deterministic results of ODEs (2.3.2) using a finite difference scheme.

As shown in Fig. (2.1), the life cycle of T. gondii involves interactions among cats, mice and environments. To investigate the significance of control process, we plot the percent of infected cats and mice in Fig. (4.1) too. We see that the population of cat converges to a steady state $N_m = 50$ (carrying capacity). The steady state does not change no matter if we use control or not. In the case of mice, the population converges to 250 without control, whereas it decreases to 220 after control. The total mouse population is decreased significantly due to implementation of control. Secondly, without control, less than one year, 75% of mice becomes infected. After 2 years, the percent of infected mice converges to a steady state 97%, which means the system approaches endemic equilibrium. Nearly every mice carries parasites. Meanwhile, it takes approximately 4.5 years for the infected mice to be significantly close to 0. In the case of cat, only 2% of them gets infected without vaccination. After implementing control process, the number of infected cats will vanish. The system goes to disease free equilibrium.

The stochastic model of (2.3.2) is also considered by us. Why do we care about stochastic model? As we mentioned in Chapter 1, some reactants may switch between favorable states stochastically such that the phenomenon cannot be fully understood if we only consider the deterministic model. In this case, a stochastic approach is necessary. In a word, the stochastic model is not only the noisy solution of the corresponding deterministic equations. Sometimes, the stochastic model might have qualitatively different properties than its deterministic limit. Fig. (4.2) shows an example given by R. Erban et al. [17] that SSA gives result which cannot be obtained by corresponding deterministic models. In Fig. (4.2), the deterministic result is represented by red line and one realization of SSA is showed by blue line. We can see that the deterministic system has only one steady state 100. However SSA shows that the fluctuations

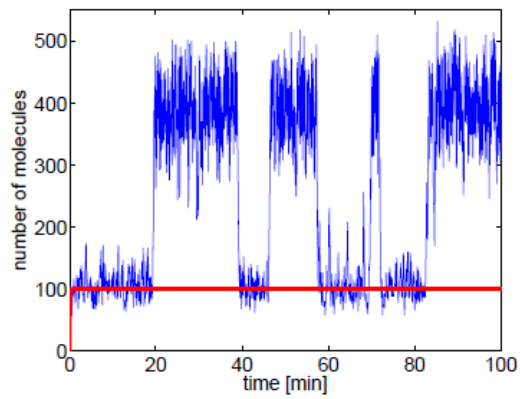

Figure 4.2: Different results between deterministic model and stochastic model [17]. The deterministic result is showed in red line and one realization of SSA is represented by blue line.

are sometimes so strong that the system spontaneously switches to another steady state 400.

Next, let us consider how to convert concentration-based differential equation regarding with E into the stochastic formulations. Remember that the variable E in our model means the proportion of contaminated environments. We also found out that the simulation results are pretty sensitive to this value. In order to implement the stochastic simulation, we need to convert the equation

$$E' = \lambda I_c - d_0 E \tag{4.1.1}$$

into reactions and calculate the corresponding reaction propensities. Let us denote the contaminated environments amount by E_b, and the total environments amount by E_T. Thus (4.1.1) is equivalent to

$$\left(\frac{E_b}{E_T}\right)' = \lambda I_c - d_0 \frac{E_b}{E_T}. \tag{4.1.2}$$

Since E_t is a constant, multiplying E_T implies that

$$E_b' = \lambda I_c E_T - d_0 E_b. \tag{4.1.3}$$

Consequently (4.1.3) can be converted into the following reactions

$$E_b \xrightarrow{d_0} \emptyset, \tag{4.1.4}$$

$$\emptyset \xrightarrow{\lambda I_c E_T} E_b. \tag{4.1.5}$$

The values of λ and d_0 are given in Table (4.2). One realization of stochastic simulation of ODEs system (2.3.2) is showed in Fig. (4.3).

The noisy fluctuations are due to the intrinsic stochasticity of the processes, including death, birth, and predator-prey events. To further reveal the stochastic effects to the system, we

Variable	Refer to	Value
λ	Environment Contamination per Cat	1/16
d_0	Environment Decontamination Rate	7/100

Table 4.2: Parameters of Environment.

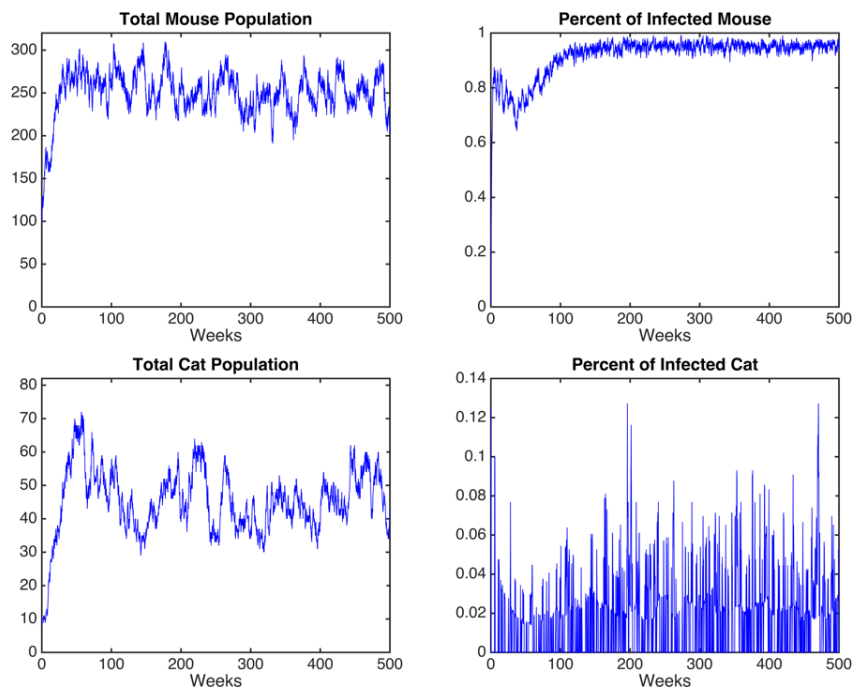

Figure 4.3: One realization of SSA for the system (2.3.2) without control.

repeat this process 500 times and collect the statistical data. The average results are showed in Fig. (4.4). In our case, we find that the stochastic mean is equal to the solution of the corresponding deterministic ODE.

In the rest part of this section, the PDEs system (2.3.3) including diffusion of hosts will be considered. We want to know if the diffusion of hosts affects the transmission dynamics of T. gondii? As we introduced, the reaction-diffusion process is key of pattern formation mechanisms in the developmental biology. Why are the reaction-diffusion processes so important? This question can be answered by a very famous problem which is called French flag problem [41]. One realization of this problem is given in Fig (4.5) [17]. Assume that one chemical A is only produced in the area $[0, 0.2]$ and the number of molecules is sensitive to the concentration of this chemical. Then the concentration gradient of A can distinguish three different regions in $[0, 1]$. Using the deterministic model, we can obtain three well-defined regions as seen in Fig. (4.5)(a). However, the fact is not as clear as what we obtained in the deterministic model. The stochastic model presents a noisy result as seen in

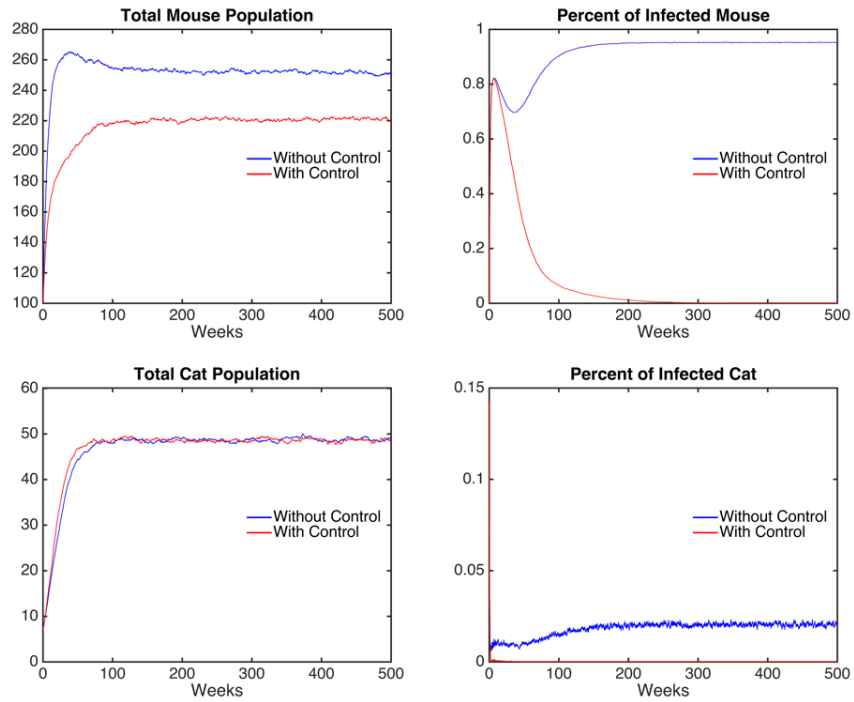

Figure 4.4: Stochastic results of ODEs (2.3.2) using SSA.

Fig. (4.5)(b). We can see that even in the area between 0 and 0.2, in which the chemical A has the highest concentration, the number of molecules may be also lower than 80. On the other hand, When we model some chemical reactions, there are only limited number of molecules involved in the reactions comparing with the large amount of total species and molecules. Consequently, the events are not enough to make average meaningful. In this case, the stochastic models provide a more detailed understanding of the reaction-diffusion processes.

In this model, we divide 1 km^2 square farm into 10×10 cells. To track the positions of the hosts as well as the distribution of oocycsts, we assign a unique coordinate for each cell. Assume that the daily activities of a cat occur in a square of 6×6 cells and the daily activities of a mouse occur in a square of 1.2×1.2 cells. The daily changes of positions of the hosts are governed by the random walk rule. Thus the diffusion rate of cats D_c is given by

$$\begin{aligned} \sqrt{2D_c} &= 6/10 \\ D_c &= 9/50\ km^2/Day \text{ or } 63/50\ km^2/Week. \end{aligned}$$

Similarly, the diffusion rate of mouse D_m is given by

$$\begin{aligned} \sqrt{2D_m} &= 1.2/10 \\ D_m &= 0.0072\ km^2/Day \text{ or } 0.05\ km^2/Week. \end{aligned}$$

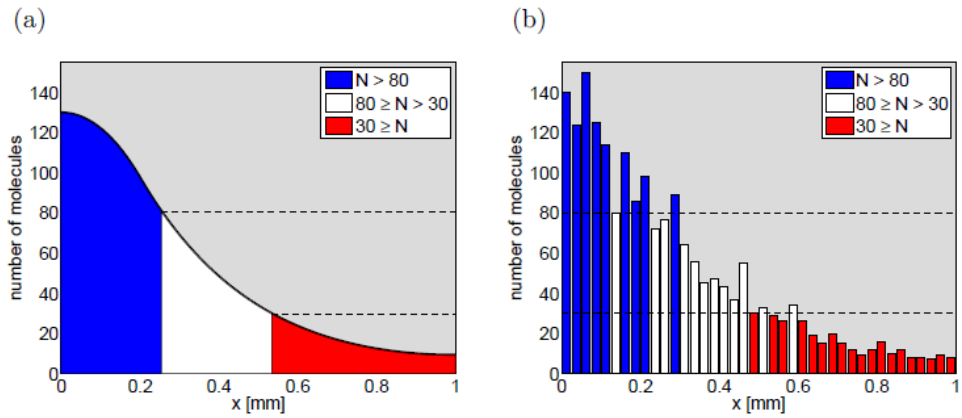

Figure 4.5: French flag problem. (a) Deterministic model. (b) Stochastic model [17].

In this thesis, we use reflective boundary conditions, that is, hosts hitting the boundary were reflected back. Such boundary conditions are suitable whenever there is no interaction between hosts in the solution and the boundary of the domain. Therefore, we have Neumann conditions $\partial_n S_c = 0$, $\partial_n I_c = 0$, $\partial_n R_c = 0$, $\partial_n S_m = 0$ and $\partial_n I_m = 0$ on each boundary. In order to do a comparison between deterministic and stochastic results of PDEs (2.3.3), we choose $E_b = 2$ and $E_T = 10$ for each compartment. All other parameters take the default values in Table (2.1), (2.2), and (4.2). Firstly, using 5-points finite difference scheme, we obtain the deterministic results which are given in Fig. (4.6). The stochastic results obtained by compartment-based model are given in Fig. (4.7). We repeat the stochastic simulation 40 times. In our case, we find that the stochastic mean is equal to the solution of the corresponding deterministic PDEs. The diffusion of hosts does not affect the transmission dynamics of the parasites. However, we may expect different results if we decrease the diffusion rate of hosts.

4.2 Parameter Effects Analysis

The reproduction number, $\mathscr{R}_0$, is a threshold parameter for a general compartmental disease transmission model based on a system of ordinary differential equations. Many epidemiological models have a Disease Free Equilibrium (DFE) at which the population remains in the absence of disease. If $\mathscr{R}_0 < 1$, then the infected population asymptotically goes to 0, and the disease cannot invade the population, whereas if $\mathscr{R}_0 > 1$, then the DFE is unstable, and invasion is always possible [23]. Here, $\mathscr{R}_0$ is the spectral radius of the Next Generation Matrix (NGM) [9]. The details about how to construct NGM will be introduced later. In the rest part of this section, we shall focus on the DFE only. In our case, the DFE means

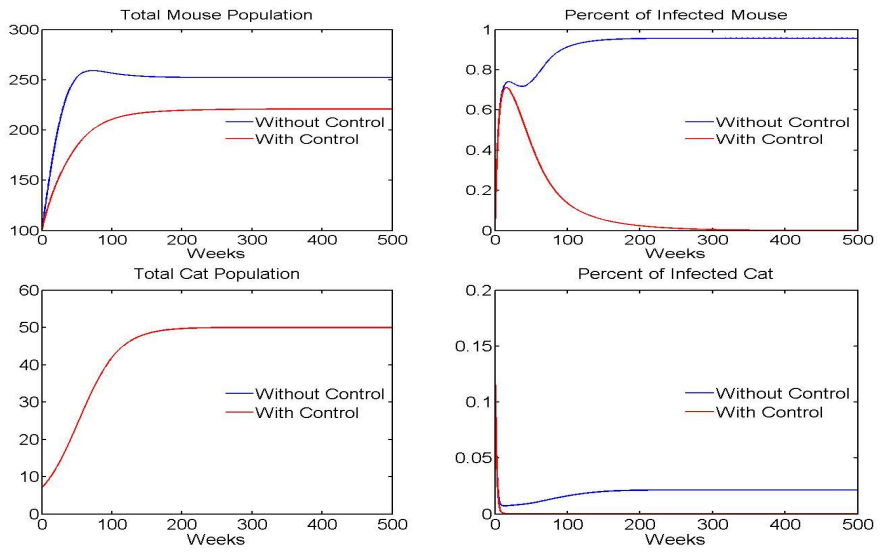

Figure 4.6: Deterministic results of PDEs (2.3.3) using finite difference scheme.

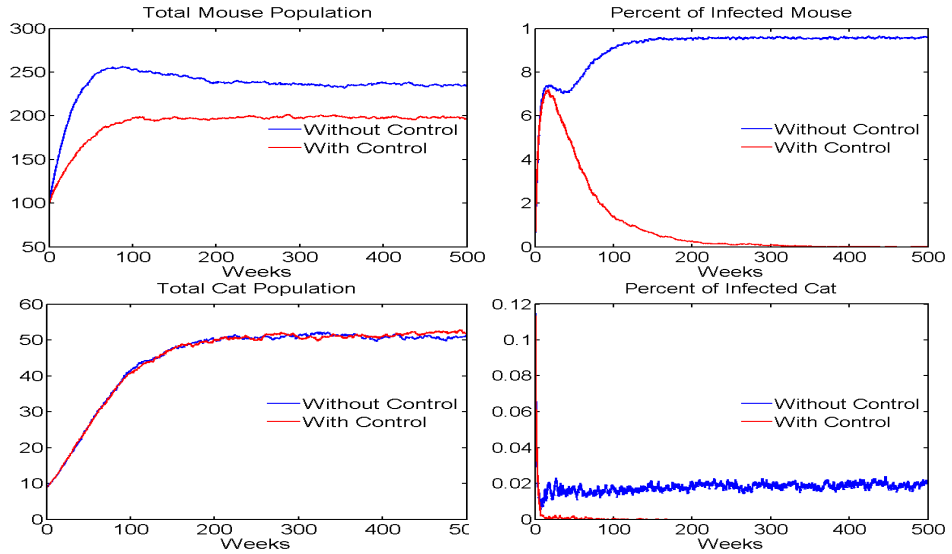

Figure 4.7: Stochatic results of PDEs (2.3.3) using SSA.

the solutions of algebra system

$$\frac{\partial I_c}{\partial t}=0,\quad \frac{\partial I_m}{\partial t}=0,\quad \frac{\partial E}{\partial t}=0,\quad \frac{\partial S_c}{\partial t}=0,\quad \frac{\partial S_m}{\partial t}=0,\quad \frac{\partial R_c}{\partial t}=0.$$

Turner. et al [34] have solved that the DFE x_0 of ODEs system (2.3.2) is

$$\begin{aligned} x_0 &= (I_c, I_m, E, S_c, S_m, R_c) \\ &= \left(0,0,0,\frac{b_cK_c}{bc+V},(r_m-\alpha K_c-H)\frac{K_m}{r_m},\frac{Vk_c}{b_c+V}\right). \end{aligned} \tag{4.2.1}$$

The basic reproduction number cannot be determined from the ODEs model alone, but also depends on the definition of infected and uninfected compartments. In order to compute $\mathscr{R}_0$, it is important to distinguish new infections from all other changes in population. Let $\mathscr{F}_i(x)$ be the rate of appearance of new infections in compartment i and $\mathscr{V}_i(x)$ be the difference between outbound individuals transfer rate and inbound individuals transfer rate of compartment i. It is assumed that both $\mathscr{F}_i(x)$ and $\mathscr{V}_i(x)$ are continuously differentiable at least twice. The disease transmission model consists of non-negative initial conditions together with the following system of equations:

$$\frac{\partial x}{\partial t}=f_i(x)=\mathscr{F}_i(x)-\mathscr{V}_i(x). \tag{4.2.2}$$

Let X be the set of all disease free states. If we assume the first m compartments correspond to infected individuals, we have

$$X=\{x\le 0|x_i=0, i=1,...,m\}.$$

Then the definition of NGM is given as follows [36]:

Definition 4.2.1. *Suppose $x_0\in X$ is a DFE of (4.2.2), the derivatives $D\mathscr{F}(x_0)$ and $D\mathscr{V}(x_0)$ are partitioned as*

$$D\mathscr{F}(x_0)=\begin{pmatrix} F & 0\\ 0 & 0\end{pmatrix},\quad D\mathscr{V}(x_0)=\begin{pmatrix} V & 0\\ J_3 & J_4\end{pmatrix},$$

where F and V are the $m\times m$ matrices defined by

$$F=\left[\frac{\partial \mathscr{F}_i}{\partial x_j}(x_0)\right]\quad \text{and}\quad V=\left[\frac{\partial \mathscr{V}_i}{\partial x_j}(x_0)\right]\quad \text{with } 1\le i,j\le m,$$

and J_3, J_4 are Jacobi Matrices. Then the NGM is defined by

$$NGM=FV^{-1}, \tag{4.2.3}$$

and basic reproduction number $\mathscr{R}_0$ is defined by

$$\mathscr{R}_0=\rho(FV^{-1}), \tag{4.2.4}$$

where ρ means the spectral radius of the matrix FV^{-1}.

Dubey [12] summarizes the recognized transmission routes of T. gondii as infection from contaminated environment, vertical transmission, and predator-prey cycle. In the remaining part, we will follow the structure of Turner's [34] work. They analyzed model (2.3.2) to discover how the parameters affect the transmission dynamics of T. gondii by calculating $\mathscr{R}_0$ of the system. Their analyses are based on deterministic model. We will check if the fluctuations can generate any differences when we assign the values near the thresholds to those corresponding parameters by adopting stochastic model. In Turner's work [34], they reduce (2.3.2) into three sub-models: Environmental infection of cats, vertical transmission in mice, and the predator-prey cycle. Meanwhile they calculate the reproduction numbers for each sub-models. Such reducing helps analysis of $\mathscr{R}_0$ of complete life cycle tremendously.

4.2.1 Transmission Cycles in Reduced Model

At first, the environmental infection of cat is considered. In this model, all mice are removed from the system. The environment is contaminated by oocysts shed by cats. The cats become infected by contacting dirty environment. The reduced model is given as follows

$$\begin{cases} \dot{S}_c = b_c N_c - \left(m_c + (b_c - m_c)\dfrac{N_c}{K_c}\right) S_c - \beta_c E S_c - V S_c \\ \dot{I}_c = -\left(m_c + (b_c - m_c)\dfrac{N_c}{K_c}\right) I_c + \beta_c E S_c - \gamma I_c \\ \dot{R}_c = -\left(m_c + (b_c - m_c)\dfrac{N_c}{K_c}\right) R_c + \gamma I_c + V S_c \\ \dot{E} = \lambda I_c - d_0 E. \end{cases} \tag{4.2.5}$$

From discussion of last section, the $\mathscr{F} - \mathscr{V}$ decomposition is given by

$$\begin{aligned} \begin{pmatrix} \dot{I}_c \\ \dot{E} \\ \dot{S}_c \\ \dot{R}_c \end{pmatrix} &= \begin{pmatrix} \beta_c E S_c \\ \lambda I_c \\ 0 \\ 0 \end{pmatrix} - \begin{pmatrix} (m_c + r_c \frac{N_c}{K_c}) I_c + \gamma I_c \\ d_0 E \\ -b_c N_c + (m_c + r_c \frac{N_c}{K_c}) S_c + \beta_c E S_c + V S_c \\ (m_c + r_c \frac{N_c}{K_c}) R_c - \gamma I_c - V S_c \end{pmatrix} \\ &= \mathscr{F} - \mathscr{V}. \end{aligned} \tag{4.2.6}$$

Note that the infection compartments should be listed in the front. Here the DFE is

$$x_0 = (I_c^*, E^*, S_c^*, R_c^*) = (0, 0, \frac{b_c K_c}{b_c + V}, \frac{V K_c}{b_c + V}). \tag{4.2.7}$$

Therefore

$$F = \begin{pmatrix} \frac{\partial \beta_c E S_c}{\partial I_c}(x_0) & \frac{\partial \lambda I_c}{\partial I_c}(x_0) \\ \frac{\partial \beta_c E S_c}{\partial E}(x_0) & \frac{\partial \lambda I_c}{\partial E}(x_0) \end{pmatrix} = \begin{pmatrix} 0 & \beta_c S_c^* \\ \lambda & 0 \end{pmatrix}, \tag{4.2.8}$$

and

$$V = \begin{pmatrix} \frac{\partial (m_c + r_c \frac{N_c}{K_c}) I_c + \gamma I_c}{\partial I_c}(x_0) & \frac{\partial (m_c + r_c \frac{N_c}{K_c}) I_c + \gamma I_c}{\partial I_c}(x_0) \\ \frac{\partial d_0 E}{\partial E}(x_0) & \frac{\partial d_0 E}{\partial E}(x_0) \end{pmatrix} = \begin{pmatrix} b_c + \gamma & 0 \\ 0 & d_0 \end{pmatrix}. \tag{4.2.9}$$

The NGM is defined as

$$\text{NGM} = FV^{-1} = \begin{pmatrix} 0 & \frac{\beta_c b_c K_c}{(b_c+V)d_0} \\ \frac{\lambda}{b_c+\gamma} & 0 \end{pmatrix}. \tag{4.2.10}$$

The basic reproduction number $\mathscr{R}_E$ of the NGM is given by

$$\mathscr{R}_E = \sqrt{\frac{\lambda\beta_c b_c K_c}{d_0(b_c+\gamma)(b_c+V)}}. \tag{4.2.11}$$

Secondly, we consider the vertical transmission in mice, i.e., the parasites are only transferred from mice to their offsprings. The reduced model is given by

$$\begin{cases} \dot{N}_c = r_c N_c \left(1 - \dfrac{N_c}{K_c}\right) \\ \dot{S}_m = b_m S_m + b_m(1-p_m)I_m - \left(m_m + (b_m - m_m)\dfrac{N_m}{K_m}\right) S_m - aN_c S_m - HS_m \\ \dot{I}_m = b_m p_m I_m - \left(m_m + \nu m_m + (b_m - m_m)\dfrac{N_m}{K_m}\right) I_m - \theta a N_c I_m - HI_m. \end{cases} \tag{4.2.12}$$

Then, the $\mathscr{F} - \mathscr{V}$ decomposition is given as follows,

$$\begin{aligned} \begin{pmatrix} \dot{I}_m \\ \dot{S}_m \end{pmatrix} &= \begin{pmatrix} b_m p_m I_m \\ 0 \end{pmatrix} - \begin{pmatrix} \left(m_m + \nu m_m + (b_m - m_m)\frac{N_m}{K_m}\right) I_m + \theta a N_c I_m + HI_m \\ -b_m S_m + b_m(1-p_m)I_m + \left(m_m + (b_m - m_m)\frac{N_m}{K_m}\right) S_m + aN_c S_m + HS_m \end{pmatrix} \\ &= \mathscr{F} - \mathscr{V} \end{aligned} \tag{4.2.13}$$

Here the DFE is

$$x_0 = (I_m^*, S_m^*) = (0, (r_m - \alpha K_c - H)\frac{K_m}{r_m}). \tag{4.2.14}$$

Therefore

$$F = \begin{pmatrix} \frac{\partial \mathscr{F}_1}{\partial I_m}(x_0) & \frac{\partial \mathscr{F}_1}{\partial S_m}(x_0) \\ \frac{\partial \mathscr{F}_2}{\partial I_m}(x_0) & \frac{\partial \mathscr{F}_2}{\partial S_m}(x_0) \end{pmatrix} = \begin{pmatrix} b_m p_m & 0 \\ 0 & 0 \end{pmatrix}, \tag{4.2.15}$$

and

$$\begin{aligned} V &= \begin{pmatrix} \frac{\partial \mathscr{V}_1}{\partial I_m}(x_0) & \frac{\partial \mathscr{V}_1}{\partial S_m}(x_0) \\ \frac{\partial \mathscr{V}_2}{\partial I_m}(x_0) & \frac{\partial \mathscr{V}_2}{\partial S_m}(x_0) \end{pmatrix} \\ &= \begin{pmatrix} \left(m_m + \nu m_m + (b_m - m_m)\frac{N_m}{K_m}\right) + \theta a N_c + H & 0 \\ b_m(1-p_m) & -b_m + \left(m_m + (b_m - m_m)\frac{N_m}{K_m}\right) + aN_c + H \end{pmatrix}. \end{aligned}$$

The basic reproduction number $\mathscr{R}_V$ of the NGM is

$$\mathscr{R}_V = \rho(FV^{-1}) = \frac{b_m p_m}{b_m - \alpha(1-\theta)K_c + \nu m_m}. \tag{4.2.16}$$

The last reduced model considers the transmission route of the predator-prey cycle. In this cycle, cats are infected by ingesting tissues of mice and mice are infected by contacting dirty environment. The reduced model is given by

$$\begin{cases} \dot{S}_c = b_c N_c - \left(m_c + (b_c - m_c)\dfrac{N_c}{K_c}\right) S_c - g(\nu)\theta a S_c I_m - V S_c \\ \dot{I}_c = -\left(m_c + (b_c - m_c)\dfrac{N_c}{K_c}\right) I_c + g(\nu)\theta a S_c I_m - \gamma I_c \\ \dot{R}_c = -\left(m_c + (b_c - m_c)\dfrac{N_c}{K_c}\right) R_c + \gamma I_c + V S_c \\ \dot{E} = \lambda I_c - d_0 E \\ \dot{S}_m = b_m N_m - \left(m_m + (b_m - m_m)\dfrac{N_m}{K_m}\right) S_m - \beta_m E S_m - a N_c S_m - H S_m \\ \dot{I}_m = -\left(m_m + \nu m_m + (b_m - m_m)\dfrac{N_m}{K_m}\right) I_m + \beta_m E S_m - \theta a N_c I_m - H I_m. \end{cases} \tag{4.2.17}$$

Here the DFE is

$$x_0 = (I_c^*, I_m^*, E^*, S_c^*, S_m^*, R_c^*) = \left(0, 0, 0, \frac{b_c K_c}{bc + V}, (r_m - \alpha K_c - H)\frac{K_m}{r_m}, \frac{V k_c}{b_c + V}\right). \tag{4.2.18}$$

The $\mathscr{F} - \mathscr{V}$ decomposition is given as follows,

$$\begin{pmatrix} \dot{I}_c \\ \dot{I}_m \\ \dot{E} \\ \dot{S}_c \\ \dot{S}_m \\ \dot{R}_c \end{pmatrix} = \mathscr{F} - \mathscr{V},$$

where

$$\mathscr{F} = \begin{pmatrix} g(\nu)\theta a S_c I_m \\ \beta_m E S_m \\ \lambda I_c \\ 0 \\ 0 \\ 0 \end{pmatrix},$$

and

$$\mathscr{V} = \begin{pmatrix} \left(m_c + (b_c - m_c)\frac{N_c}{K_c}\right) I_c + \gamma I_c \\ \left(m_m + \nu m_m + (b_m - m_m)\frac{N_m}{K_m}\right) I_m + \theta a N_c I_m + H I_m d_0 E \\ -(b_c N_c - \left(m_c + (b_c - m_c)\frac{N_c}{K_c}\right) S_c - g(\nu)\theta a S_c I_m - V S_c) \\ -(b_m N_m - \left(m_m + (b_m - m_m)\frac{N_m}{K_m}\right) S_m - \beta_m E S_m - a N_c S_m - H S_m) \\ -(-\left(m_c + (b_c - m_c)\frac{N_c}{K_c}\right) R_c + \gamma I_c + V S_c) \end{pmatrix}.$$

Therefore

$$F = \begin{pmatrix} 0 & g(\nu)\theta\alpha S_c I_m & 0 \\ 0 & 0 & \beta_m S_m \\ \lambda & 0 & 0 \end{pmatrix}, \tag{4.2.19}$$

and

$$V = \begin{pmatrix} b_c + \gamma & 0 & 0 \\ m_m + \nu m_m + (b_m - m_m)\frac{r_m - \alpha K_c - H}{r_m} & 0 & H I_m d_0 \\ 0 & -g(\nu)\theta a S_c & 0 \end{pmatrix}. \tag{4.2.20}$$

The NGM is given by

$$\text{NGM} = FV^{-1} = \begin{pmatrix} 0 & 0 & \frac{g\theta\alpha b_c K_c}{(b_c+V)(b_m-\alpha(1-\theta)K_c+\nu m_m)} \\ \frac{\lambda}{b_c+\gamma} & 0 & 0 \\ 0 & \frac{\beta_m(r_m-\alpha K_c-H)\frac{K_m}{r_m}}{d_0} & 0 \end{pmatrix}. \tag{4.2.21}$$

Finally, the basic reproduction number of this reduced model is

$$\mathscr{R}_P = \left(\frac{\beta_m K_m^* \lambda g\theta\alpha b_c K_c}{d_0(b_c+\gamma)(b_c+V)(b_m - \alpha(1-\theta)K_c + \nu m_m)} \right)^{1/3}, \tag{4.2.22}$$

where

$$K_m^* = \frac{(r_m - \alpha K_c - H)K_m}{r_m}.$$

For the complete life cycle, the basic reproduction number $\mathscr{R}_0$ is the largest magnitude among the roots of the following equation

$$f(R) = R^3 - \mathscr{R}_V R^2 - \mathscr{R}_E^2 R - \mathscr{R}_P^3 + \mathscr{R}_V \mathscr{R}_E^2. \tag{4.2.23}$$

The above results are as same as Turner's work [34]. They also show that if infection persists in any reduced model, it persists in the complete life cycle, i.e.,

$$\mathscr{R}_0 \geq Max(\mathscr{R}_E, \mathscr{R}_V, \mathscr{R}_P). \tag{4.2.24}$$

In next section, we will apply Gillespie SSA to simulate this complete life cycle at those values near the thresholds. The purpose is to investigate if the stochastic model agrees with the analyses based on the deterministic model and see if the fluctuations generate any differences near those thresholds.

4.2.2 Parameter Effects

Carrying Capacity Kc and Cat Vaccination Rate V

Combining (4.2.11), (4.2.16), and (4.2.22) implies that

$$\frac{\mathscr{R}_P^3}{\mathscr{R}_E^2 \mathscr{R}_V} = \frac{\beta_m g\theta\alpha(r_m - \alpha K_c - H)K_m^*}{\beta_c b_m p_m r_m}. \tag{4.2.25}$$

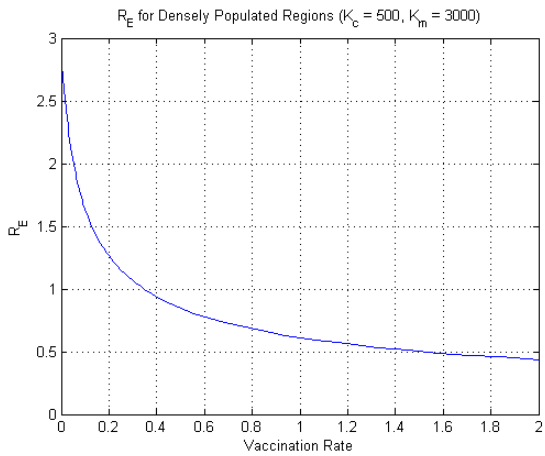

Figure 4.8: The correlation of $\mathscr{R}_E$ and V in densely populated region with $K_c = 500$ and $K_m = 3000$.

Note that if the carrying capacity of cat, K_c, is increased, the quotient (4.2.25) decreases. In another word, the significance of $\mathscr{R}_E$ and $\mathscr{R}_V$ is improved by raising the carrying capacity of cat, K_c. On the other hand, if we set behavioral change parameter $\theta > 1$, $\mathscr{R}_V$ would be a decreasing function in K_c. Therefore if K_c is increased, the environment contamination cycle will be the most important part to affect complete life cycle of transmission. Consequently, we turn our focus on $\mathscr{R}_E$ first.

From (4.2.11), we see that $\mathscr{R}_E$ is a decreasing function for any $V > 0$. Intuitively, in those densely populated regions, the vaccination of cat cannot eliminate the transmission of parasite. This result is easily verified by enhancing the carrying capacity of cat, Kc. To make it more realistic, I also raises carrying capacity of mouse, K_m. Although this may increase the effects of $\mathscr{R}_P$. In order to investigate the correlation between $\mathscr{R}_E$ and vaccination rate V in those densely populated regions, we set $K_c = 500$ and $K_m = 3000$. The reason why we choose such big numbers is to make the threshold of $V > 0$. The function $\mathscr{R}_E$ in V is given in Fig. (4.8). Note that if $V < 0.3456$, the basic reproduction number, $\mathscr{R}_E > 1$. Consequently, (4.2.24) implies that $\mathscr{R}_0 > 1$ too which means the system approaches endemic equilibrium rather than DFE. Let $V = 0.3$, a value smaller than and near 0.3456. We simulate this case to investigate if this property agrees with the stochastic model. The stochastic simulation using Gillespie SSA is given in Fig. (4.9). As we know, $V = 0.3$ is sufficient to make the system approach DFE asymptotically in the sparsely populated regions. However, in this case, for those densely populated regions, both infected cats and infected mice approach endemic equilibrium. The vaccination of cat cannot control the endemic of infection.

In the last simulation, we investigate the stochastic model near the threshold of V such that $\mathscr{R}_E > 1$. Next, we turn our focus on $\mathscr{R}_0$. Actually, the threshold of carrying capacity such that $\mathscr{R}_0 > 1$ is not necessarily high as we choose in Fig. (4.9). Suppose that the vaccination rate is fixed, the value of basic reproductive number $\mathscr{R}_0$ is controlled by the

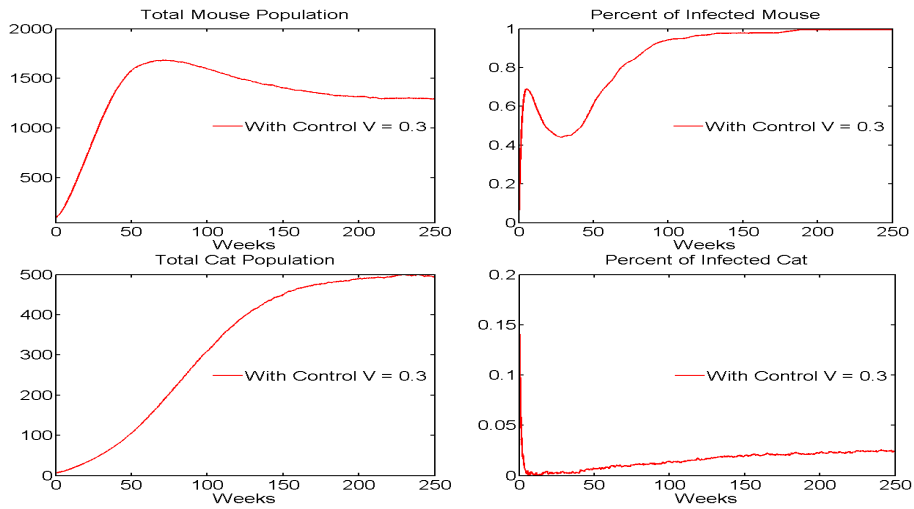

Figure 4.9: Stochastic results of (2.3.2) in densely populated regions with $K_c = 500$ and $K_m = 3000$. All other parameters take the default values in Chapter 2.

carrying capacity of cat K_c. The graphs of $\mathscr{R}_0$, $\mathscr{R}_P$ and $\mathscr{R}_V$ in variable V are given in Fig. (4.10). If we choose $V = 0.3$, the threshold of K_c such that $\mathscr{R}_0 > 1$ is near 47. In case (b), the threshold raises to 103 after increasing V to 0.7. We simulate case (a) by using Gillespie SSA and choosing $K_c = 47$. The results are given in (4.11).

Considering Fig. (4.11), if K_c surpasses the threshold 46.5, under the control with $H = 1/52$ and $V = 0.3$, the system approaches endemic equilibrium rather than disease free equilibrium. The percent of infected mice goes to 12% after 150 weeks. For cats, the simulation result is not apparent. But, at least we can see that the infected cats do not disappear. This results agree with the corresponding deterministic analyses. The histogram of the infected percentage of the stochastic model at $t = 200$ is given in Fig. (4.12). The mean percent of infected mice is around 12%. For the percent of infected cats, most of the trajectories go to zero, and some go to 2%.

In Fig. (4.13), we only focus on the transmission under control. The carrying capacity K_c is increased to 103 which is over the threshold such that $\mathscr{R}_0 < 1$ when choosing $V = 0.7$. Here, we assign two different values, $V = 0.3$ and $V = 0.7$, to vaccination rate of cat. The purpose is to investigate the effect of V on parasite's transmission dynamics. Both cases are under control with $H = 1/52$. The blue line represents the case with lower vaccination rate $V = 0.3$. Correspondingly, the case with higher vaccination rate $V = 0.7$ is represented by red line. In this result, we can see that, near the threshold value of K_c, the infection percentage also decreases after raising the vaccination rate in the stochastic model. Especially for mice, the infection percentage decreases from 60% to 10%. Consequently, we confirm that the increasing of vaccination rate can restrain the infection percentage of hosts which is consistent with the deterministic analysis. However, the effects of vaccination in densely populated

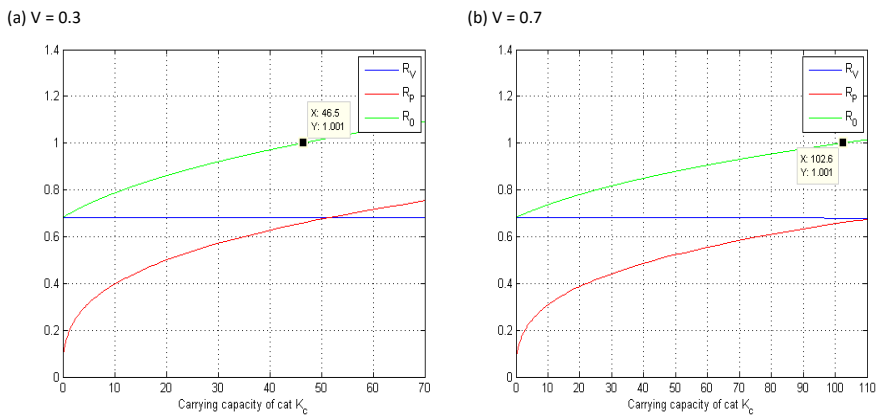

Figure 4.10: The graphs of $\mathscr{R}_V$, $\mathscr{R}_P$ and $\mathscr{R}_0$ in variable K_c. (a) The vaccination rate $V = 0.3$. (b) The vaccination rate $V = 0.7$. All other parameters take the default values in Chapter 2.

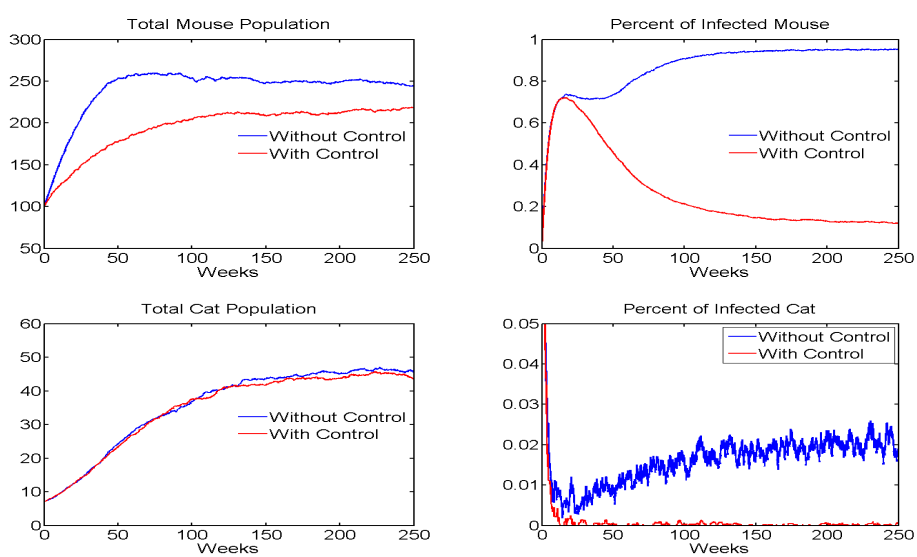

Figure 4.11: The stochastic simulation of transmission with $V = 0.3$, $H = 1/52$. Here we choose carrying capacity of cat, $K_c = 47$. All other parameters take the default values in Chapter 2.

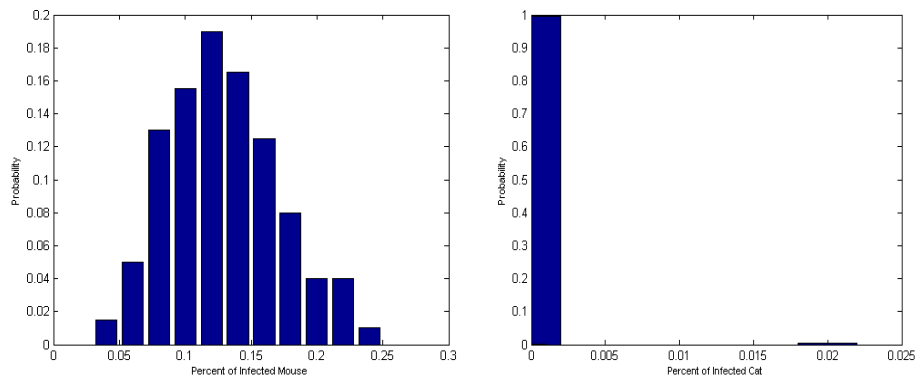

Figure 4.12: The histogram of the infected percentage of stochastic model at $t = 200$ with control $V = 0.3$, $H = 1/52$. Here we choose carrying capacity of cat, $K_c = 47$. All other parameters take the default values in Chapter 2.

regions is limited. With increasing of carrying capacity K_c, the effects of vaccination V on $\mathscr{R}_0$ will be weakened.

Predation Rate α

If we consider (4.2.25) as a function in predation rate α, we can draw it as a concave down parabola, see Fig. (4.14). We can see that the vertex is around 0.0006. When predation rate α goes from 0 to 0.0006, the significance of the predation-prey cycle is increased, comparing with the other two cycles. However, when α surpasses this threshold, the increasing α may suppress the number of mice such that the influences of predation-prey cycle decrease. In this case, efficient vertical transmission and environmental contamination become more important to sustain the transmission.

Note that both $\mathscr{R}_V$ (4.2.16) and $\mathscr{R}_P$ (4.2.22) depend on parameter α. Let $\theta = 1.2$, then the denominator of $\mathscr{R}_V$ is always positive and $\mathscr{R}_V$ is a decreasing function in α. The basic reproductive rate of complete life cycle, $\mathscr{R}_0$, can be calculated by (4.2.23). The graphs of $\mathscr{R}_V$, $\mathscr{R}_P$ and $\mathscr{R}_0$ in α are given in Fig. (4.13). In this picture, the rate of the predation-prey cycle, $\mathscr{R}_P$, and the rate of the complete life cycle, $\mathscr{R}_0$, have a pretty similar arc-shape graph, which means the parameter α affects the transmission mainly through the predation - prey cycle. Actually, if $\theta > 1$, the basic reproductive number $\mathscr{R}_V$ of the vertical transmission cycle is always lower than one. Consequently, the influence of α in the vertical transmission cycle can be ignored. We see that the rate $\mathscr{R}_0$ first surpasses the threshold 1 near $\alpha = 4e-5$. Based on the definition, if $\mathscr{R}_0 > 1$, the system cannot approach DFE asymptotically. Then

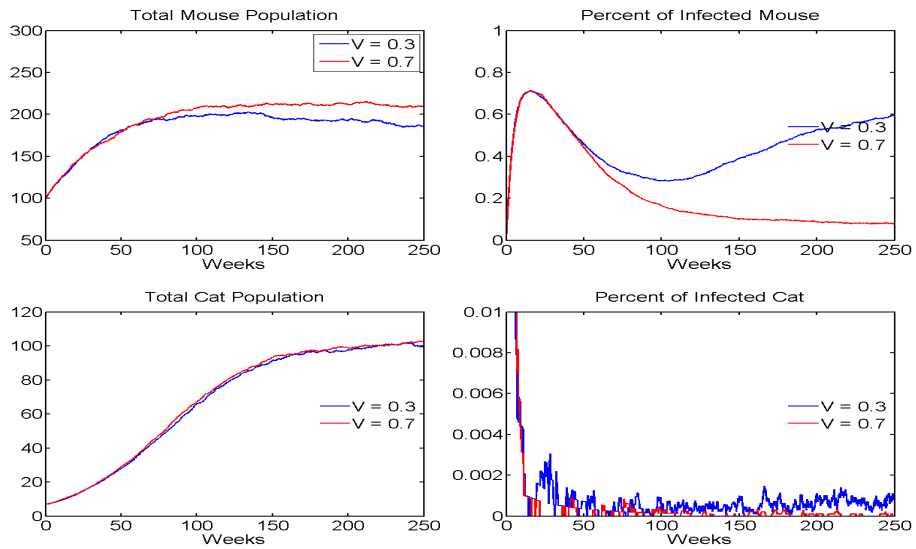

Figure 4.13: Stochastic results of two different vaccination rates in densely populated regions with $K_c = 103$ and $K_m = 300$. All other parameters take the default values in Chapter 2.

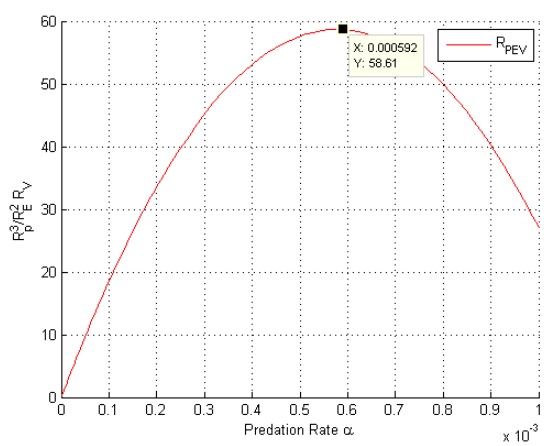

Figure 4.14: The graph of function $\frac{\mathscr{R}_P^3}{\mathscr{R}_E^2 \mathscr{R}_V}$ in variable α. All parameters take the default values in Chapter 2.

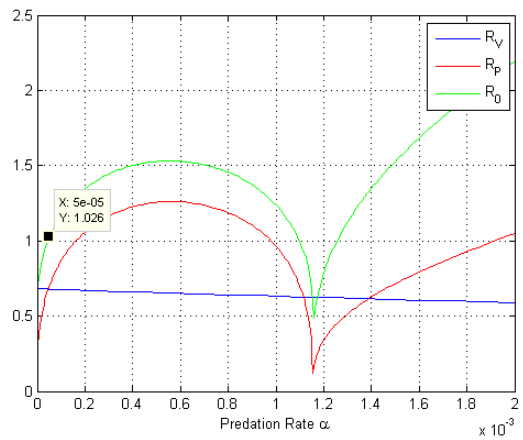

Figure 4.15: The graphs of $\mathscr{R}_V$, $\mathscr{R}_P$ and $\mathscr{R}_0$ in variable α. All parameters take the default values in Chapter 2.

we choose $\alpha = 5e-5$ to check if the stochastic model has the same property. The simulation result is given in Fig. (4.16).

In Fig. (4.15), $\mathscr{R}_0$ surpasses the threshold 1 when $\alpha = 5e-5$. Comparing with the results showed in Fig. (4.4) where $\alpha = 2e-5$, since the change is pretty tiny, we see that the equilibrium of population is not affected. But the percentage of infected mice approaches 20% rather than 0 even under control, i.e., the system goes to endemic equilibrium state asymptotically. This result agrees with our analysis. The histogram of this simulation at $t = 200$ is given in Fig. (4.17). Next, we increase the α to $5e-4$, the value which is close to the position of critical point of $\mathscr{R}_0$. The stochastic simulations are given in Fig. (4.18). In this simulation, we see that the increasing α reduces the population of mice sharply. Meanwhile, the percent of infected mice raises to almost 80% even under control. The stochastic model shows that the predation parameter α is the crucial factor for the transmission dynamics. It not only restrains the population of mice. When α is lower than the critical value, the infection percentage is raised with increasing of α.

Finally, Let us observe the change of infected percentage with different values of parameter α. We increase the α to a higher value $1e-3$ and compare the time evolution trajectories of infection percentage with three different predation rates. The comparison based on deterministic model is showed in Fig. (4.19). In this comparison, only those transmissions with vaccination and harvesting control are considered. We assign 3 different values to the predation rate α. The blue line represents the case with $\alpha = 5e-5$, which is near the threshold point when $\mathscr{R}_0$ just surpasses 1. The red line represents the trajectory with $\alpha = 5e-4$, which is near the vertex of $\mathscr{R}_0$. The last trajectory with $\alpha = 1e-3$ is represented by green line. At this value of α, $\mathscr{R}_0$ has been surpassed the vertex but is still greater than 1. The values of α are chosen by increasing order. When α is just over $5e-5$, meanwhile $\mathscr{R}_0$ strides over the threshold, the disease starts to be uncontrollable. However, the situation is not serious. Only

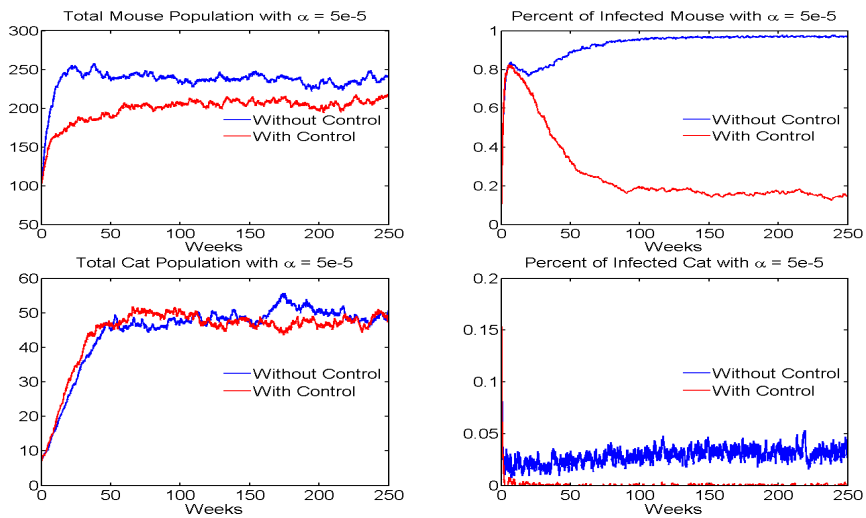

Figure 4.16: The stochastic simulation of transmission. Here we choose predation rate $\alpha = 5e - 5$. All other parameters take the default values in Chapter 2.

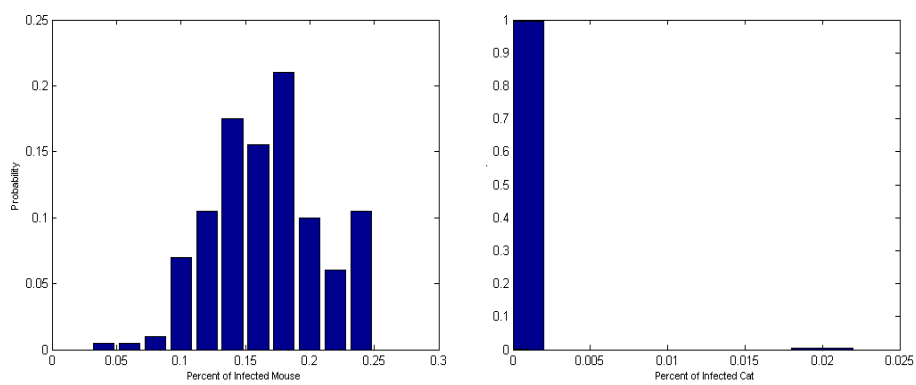

Figure 4.17: The histogram of the infected percentage of stochastic model under control at $t = 200$. Here we choose predation rate $\alpha = 5e - 5$. All other parameters take the default values in Chapter 2.

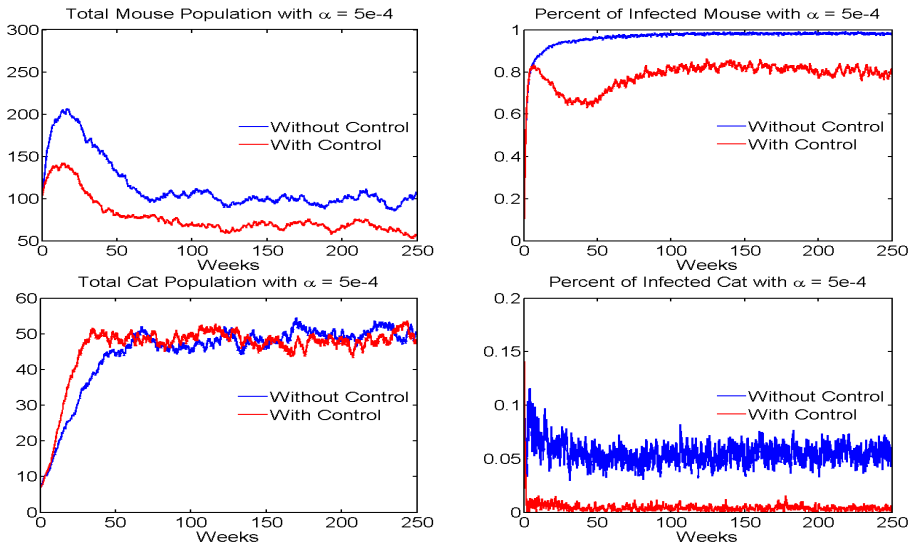

Figure 4.18: The stochastic simulation of transmission. Here we choose predation rate $\alpha = 5e - 4$. All other parameters take the default values in Chapter 2.

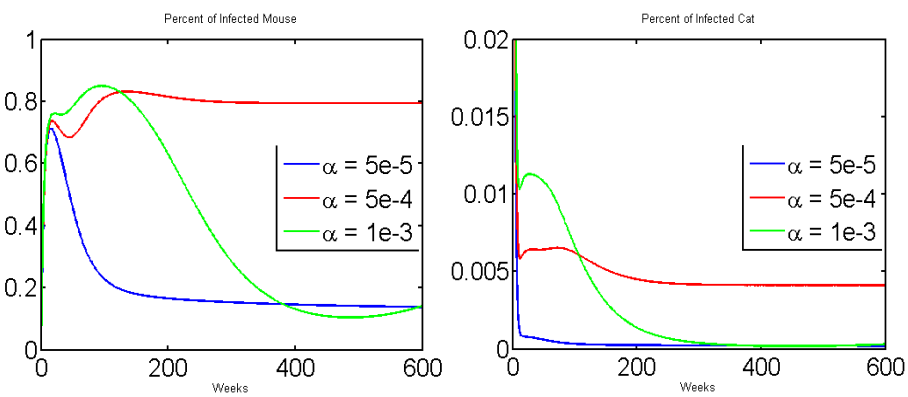

Figure 4.19: The comparison of transmission dynamics with different α under control. Here we choose predation rate $\alpha = 5e - 5$, $\alpha = 5e - 4$, and $\alpha = 1e - 3$ respectively. All other parameters take the default values in Chapter 2.

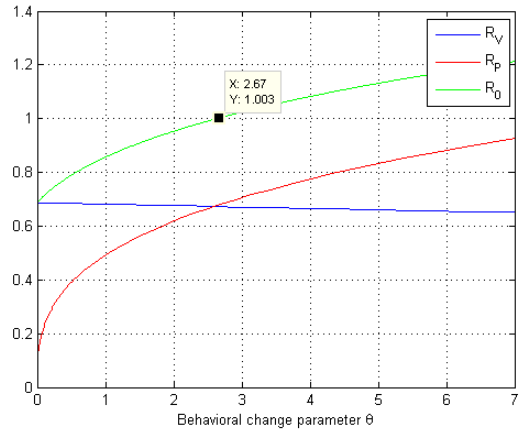

Figure 4.20: $\mathscr{R}_V$, $\mathscr{R}_P$ and $\mathscr{R}_0$ of θ. All parameters take the default values in Chapter 2.

nearly 20% of mice get infected and the infection of cats can be almost eliminated. After increasing α to $5e-4$, where $\mathscr{R}_0$ touches its maximum, the infection is increased to be more terrible. The increasing α implies the higher level prevalence of the transmission. Nearly 80% of mice and 0.5% of cats become infected. The control method is no longer workable even we increase the value of V and H. However, if we continue raising the α to a higher lever $1e-3$, from Fig. (4.15), we find that the reproductive rate $\mathscr{R}_0$ decreases to a lower level. When predation rate surpasses the critical point, predation becomes so frequent as to suppress the predator-prey cycle by removing too many intermediate hosts. Consequently, the predator-prey cycle is weakened and the percent of infected mice decreases to 20% again. These results are consistent with our stochastic model.

Behavioral Change Rate θ

As we discussed in Chapter 2, the behavior of mice may be changed after infection. This phenomenon is modeled in system (2.3.2) by parameter θ. In the system, the mice are preyed upon at a natural predation rate αN_c. After introducing θ, the rate $\theta\alpha N_c$ may vary. The predation rate will be raised if $\theta > 1$ which means the infection alters the mouse's behavior such that it is more prone to becoming prey. If $\theta < 1$, the infected mouse is more prone to avoiding cat. In this case the infection would increase the survival of its intermediate host. Hence infection could persist in mice. The correlation between basic reproduction numbers and θ is given in Fig. (4.20). Note that the reproductive rate $\mathscr{R}_V$ of vertical transmission cycle is an increasing function when $0 < \theta < 1$, even it is not clear in the figure since the predation rate α is pretty small. If we only consider vertical transmission path, avoiding predation could be a better choice for the transmission of T. gondii. When $\theta > 1$, $\mathscr{R}_V$ is monotone decreasing in θ. Based on the parameters we choose, the vertical transmission cycle always goes to DFE. In Fig. (4.18), $\mathscr{R}_P$ and $\mathscr{R}_0$ form a very similar shape, i.e. the

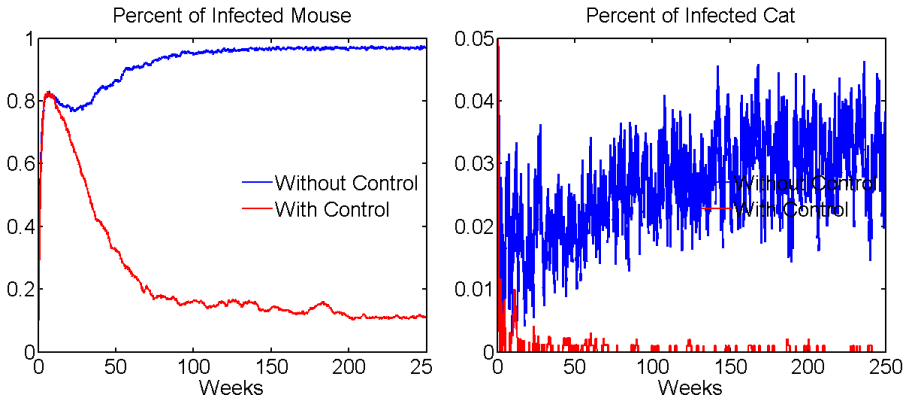

Figure 4.21: The stochastic simulation of transmission. Here we choose behavior change parameter $\theta = 2.7$. All other parameters take the default values in Chapter 2.

predator-prey cycle may dominate the complete life cycle for those parameters chosen by us. $\theta = 2.67$ is the first position where $\mathscr{R}_0$ surpasses the threshold 1. We apply Gillespie SSA to simulate the system using this value to investigate if the stochastic result agrees with our analysis. The simulation result is showed in Fig. (4.21). In this simulation, after raising the value of θ to 2.7, we see that the percentage of infected mice asymptotically approaches 12% rather then disappearance. For cat, the result is not apparent, but we can confirm that the equilibrium is not 0. The corresponding histogram at $t = 200$ is given in Fig. (4.22).

4.3 The Model Including Sheep

In the last section, we consider a more complex model including herbivore end receiver, sheep. We assume that sheep develop life-long infections. Then we split total sheep population N_s into two parts, S_s and I_s, representing the numbers of susceptible and infected sheep. The population of sheep grow logistically with intrinsic growth rate $r_s = b_s - m_s$, where b_s is the nature birth rate and m_s is the nature mortality rate. Sheep may be infected in either of two ways. Firstly, sheep are infected by contaminated environment with transmission rate β_s. Secondly, sheep are also infected by vertical transmission with rate p_s. Let K_s denote the carrying capacity of sheep, the transmission dynamics of sheep is described by the following

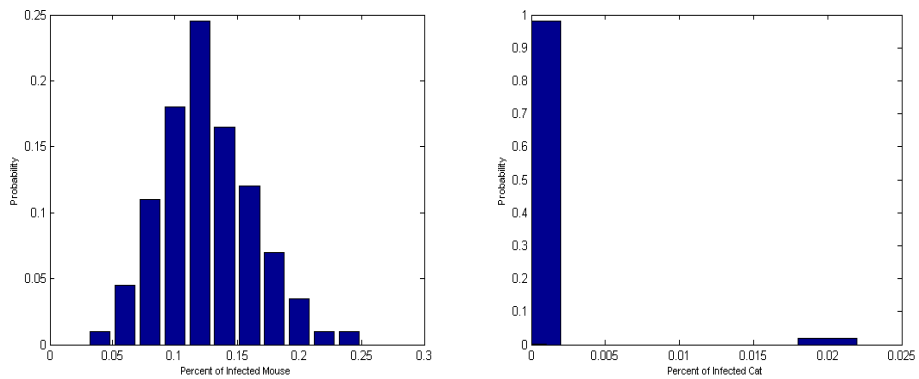

Figure 4.22: Histogram of the infected percentage of stochastic model under control at $t = 200$. Here we choose behavior change parameter $\theta = 2.7$. All other parameters take the default values in Chapter 2.

Variable	Refer to	Value
b_s	Sheep Birth Rate	1.6/52
m_s	Sheep Death Rate	0.6/52
r_s	$r_s = b_s - m_s$	1/52
β_s	Environment Transmission Rate to Sheep	0.5
K_s	Sheep Carrying Capacity	100
p_s	Vertical Transmission Probability	0.69

Table 4.3: Parameters of Sheep.

ODEs system,

$$\begin{cases} \dot{S}_s = b_s S_s + b_s(1-p_s)I_s - \left(m_s + (b_s - m_s)\dfrac{N_s}{K_s}\right) S_s - \beta_s E S_s, \\ \dot{I}_s = b_s p_s I_s - \left(m_s + (b_s - m_s)\dfrac{N_s}{K_s}\right) I_s + \beta_s E S_s. \end{cases} \tag{4.3.1}$$

The values of parameters are collected from [40] and listed in Table (4.3). We can also convert this deterministic model into the stochastic formulations. The reactions and corresponding propensity functions are listed in Table (4.4).

Transition	Reaction	Propensity
S_s generation from S_s	$S_s \xrightarrow{b_s} 2S_s$	$\alpha_{19} = b_s S_s$
S_s generation from I_s	$I_s \xrightarrow{b_s(1-p_s)} I_s + S_s$	$\alpha_{20} = (b_s(1-p_s))\, I_s$
S_s degradation	$S_s \xrightarrow{m_s + r_s \frac{N_s}{K_s}} \emptyset$	$\alpha_{21} = \left(m_s + r_s \frac{N_s}{K_s}\right) S_s$
S_s to I_s by E	$S_s \xrightarrow{\beta_s E} I_s$	$\alpha_{22} = \beta_s E S_s$
I_s generation	$I_s \xrightarrow{b_s p_s} 2I_s$	$\alpha_{23} = b_s p_s I_s$
I_s degradation	$I_s \xrightarrow{m_s + r_s \frac{N_s}{K_s}} \emptyset$	$\alpha_{24} = \left(m_s + r_s \frac{N_s}{K_s}\right) I_s$

Table 4.4: Stochastic Formulations and Propensity Functions of Sheep.

Variable	Refer to	Initial Value
S_s	Number of Susceptible Sheep	20
I_s	Number of Infected Sheep	0

Table 4.5: Initial Values of Sheep.

Next, we incorporate (4.3.1) into (2.3.2) to form a complex life cycle of transmission which is more realistic to the real farm.

$$\begin{cases} \dot{S}_c = b_c N_c - \left(m_c + (b_c - m_c)\dfrac{N_c}{K_c}\right) S_c - \beta_c E S_c - g(\nu)\theta a S_c I_m - V S_c \\ \dot{I}_c = -\left(m_c + (b_c - m_c)\dfrac{N_c}{K_c}\right) I_c + \beta_c E S_c + g(\nu)\theta a S_c I_m - \gamma I_c \\ \dot{R}_c = -\left(m_c + (b_c - m_c)\dfrac{N_c}{K_c}\right) R_c + \gamma I_c + V S_c \\ \dot{E} = \lambda I_c - d_0 E \\ \dot{S}_m = b_m S_m + b_m(1-p_m) I_m - \left(m_m + (b_m - m_m)\dfrac{N_m}{K_m}\right) S_m - \beta_m E S_m - a N_c S_m - H S_m \\ \dot{I}_m = b_m p_m I_m - \left(m_m + \nu m_m + (b_m - m_m)\dfrac{N_m}{K_m}\right) I_m + \beta_m E S_m - \theta a N_c I_m - H I_m \\ \dot{S}_s = b_s S_s + b_s(1-p_s) I_s - \left(m_s + (b_s - m_s)\dfrac{N_s}{K_s}\right) S_s - \beta_s E S_s \\ \dot{I}_s = b_s p_s I_s - \left(m_s + (b_s - m_s)\dfrac{N_s}{K_s}\right) I_s + \beta_s E S_s. \end{cases} \tag{4.3.2}$$

Using the initial value given in Table (4.5), the concentration based deterministic simulation of this system is given in Fig. (4.23). The result shows the time evolution trajectories of population and infection rate of sheep. We can see that under vaccination and harvesting control, after 12 years, the system approaches DFE asymptotically, i.e., the transmission of parasite in sheep can be eliminated by implementation of control process on cats and mice.

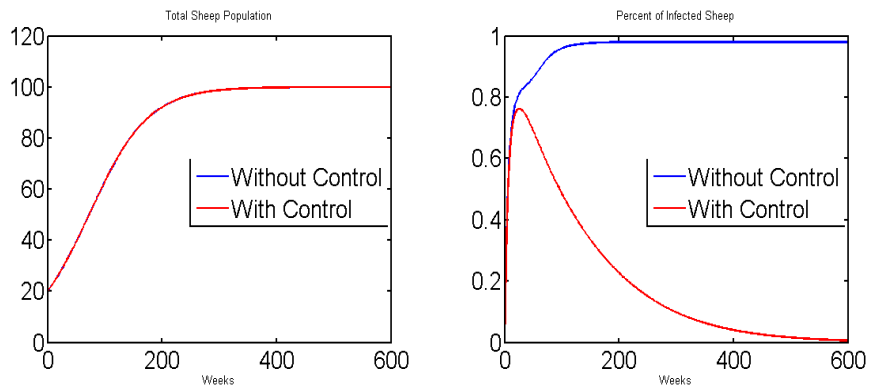

Figure 4.23: The deterministic simulation of sheep.

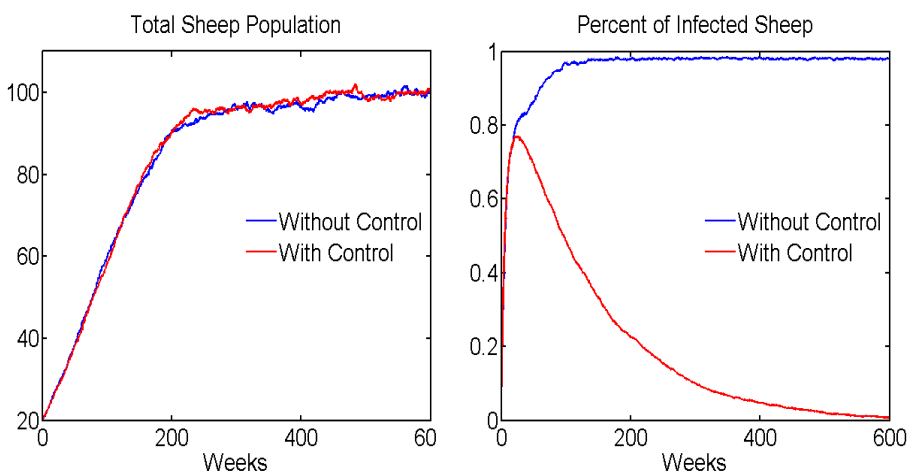

Figure 4.24: The stochastic simulation of sheep.

The stochastic model also verifies this result which is given in Fig. (4.24). The DFE of (4.3.2) is

$$x_0 = (I_c^*, I_m^*, E^*, I_s^*, S_c^*, S_m^*, R_c^*, S_s^*) = \left(0, 0, 0, 0, \frac{b_c K_c}{bc + V}, (r_m - \alpha K_c - H)\frac{K_m}{r_m}, \frac{V k_c}{b_c + V}, K_s\right). \tag{4.3.3}$$

Turner et. al[34] have shown that the basic reproduction number $\mathscr{R}_{s0}$ of (4.3.2) is the largest magnitude among the roots of following characteristic function

$$f(R) = (R^3 - \mathscr{R}_V R^2 - \mathscr{R}_E^2 R - \mathscr{R}_P^3 + \mathscr{R}_V \mathscr{R}_E^2)(p_s - R). \tag{4.3.4}$$

Note that the first part is as same as (4.2.23). Since the vertical transmission rate p_s cannot be greater than 1, the analyses based on cats-mice model are still workable on this complex model. In another word, any parameter such that $R_0 > 1$ also makes (4.3.2) go to endemic equilibrium.

Bibliography

[1] E. Afonso, M. Lemoine, M.L. Poulle, M.C. Ravat, S. Romand, P. Thulliez, I. Villena, D. Aubert, M. Rabilloud, B. Riche, E. Gilot-Fronmont, Spatial distribution of soil contamination by Toxoplasma gondii in relation to cat defecation behaviour in an urban area, *International Journal for Parasitology* 38(8-9), 1017-1023, 2008.

[2] E. Afonso, P. Thulliez, E. Gilot-Fronmont, Transmission of Toxoplasma gondii in an urban population of domestic cats(Felis catus), *International Journal for Parasitology* 36(13), 1373-1382, 2006.

[3] E. Afonso, P. Thulliez, P. Pontier, E. Gilot-Fronmont, Toxoplasmosis in prey species and consequences for prevalence in feral cats: not all prey species are equal, *Parasitology* 134, 1963-1971, 2007.

[4] S.S. Andrews, D. Bray, Stochastic simulation of chemical reactions with spatial resolution and single molecule detail, *Physical Biology 1* 137-151, 2004.

[5] A.J. Arenas, G. González-Parra, R.J.V. Micó, Modeling toxoplasmosis spread in cat populations under vaccination, *Theoretical Population Biology* 77, 227-237, 2010.

[6] M.B. Batz, S. Hoffmann, M.J. Glenn, Ranking the risks: the 10 pathogen-food combinations with the greatest burden on public health, *Thechnical Report* Emerging Pathogens Institute, University of Florida, 2011.

[7] H. Berg, Random Walks in Biology, *Princeton University Press*, 1983.

[8] F. Courchamp, D. Pontier, M. Langlais, M. Artois, Population dynamics of Feline Immunodeficiency Virus within cat populations, *Journal of Theoretical Biology* 175(4), 553-560, 1995.

[9] O. Diekmann, J.A.P. Heesterbeek, J.A.J. Metz, On the definition and the computation of the basic reproduction ratio $\mathscr{R}_0$ in models for infectious diseases in heterogeneous populations, J. Math. Biol. 28(1990)365.

[10] J.P. Dubey, Tissue cyst tropism in Toxoplasma gondii: a comparison of tissue cyst formation in organs of cats, and rodents fed oocysts, *Parasitology* 115, 15-20, 1997.

[11] J.P. Dubey, Comparative infectivity of oocysts and bradyzoites of Toxoplasma gondii for intermediate(mice) and definitive(cats) hosts, *Veterinary Parasitology* 140(1-2), 69-75, 2006.

[12] J.P. Dubey, History of the discovery of the life cycle of toxoplasma gondii, *International Journal for Parasitology* 39, 877-882 2009.

[13] J.P. Dubey, Toxoplasmosis of Animals and Humans, second edition, *CRC Press*, 2009.

[14] J.P. Dubey, Toxoplasmosis of Animals and Man, first edition, *CRC Press*, 2010.

[15] A. Dumetre, M.L. Darde, How to detect Toxoplasma gondii oocysts in environmental samples? *Fems Microbiology Reviews* 27(5), 651-661, 2003.

[16] A. Einstein, Investigations on the theory of the Brownian movement, *Dover Publications Inc*, 1967

[17] R. Erban, S. Chapman, and P.K. Maini, A practical guide to stochastic simulations of reaction-diffusion processes, *arxiv.org/pdf/0704.1908* 2007.

[18] D. Fangem O.G. Berg, P. Sjberg, and J. Elf, Stochastic reaction-diffusion kinetics in the microscopic limit, *National Academy of Sciences*, 107(46):19820-19825, 2010

[19] C. Gardiner, K. McNeil, D. Walls, and I. Matheson, Correlations in stochastic theories of chemical reactions, *Journal of Statistical Physics*, 14:307-331, 1976.

[20] M.Gibson, and J. Bruck, Efficient exact stochastic simulation of chemical systems with many species and many channels, *Journal of Physical Chemistry A*,102(2000), 1876-1889

[21] D. Gillespie, A General Method for Numerically simulating the stochastic time evolution of coupled chemical reactions, *Journal of Computational Physics*, 1976.

[22] D. Gillespie, Exact stochastic simulation of coupled chemical reactions, *The Journal of Physical Chemistry*, 81, 25 (1977), 2340 - 2361.

[23] H.W. Hethcote, The mathematics of infectious diseases, *SIAM Rev.* 42, 599, 2000.

[24] G. Hide, E.K. Morley, J.M. Hughes, O. Gerwash, M.S. Elmahaishi, K.H. Elmahaishi, D. Thomasson, E.A. Wright, R.H. Williams, R.G. Murphy, J.E. Smith, Evidence for high levels of vertical transmission in Toxoplasma gondii, *Parasitology* 136, 1877-1885, 2009.

[25] W. Jiang, A.M. Sullivan, C. Su, X. Zhao, An agent-based model for the transmission dynamics of Toxoplasma gondii, *Hournal of Theoretical Biology*, 293, 15-26, 2012.

[26] M. Lélu, M. Langlais, M.L. Poulle, E. Gilot-Fromont, Transmission dynamics of toxoplasma gondii along an urban-rural gradient, *Theoretical Population Biology* 139-147, 2010.

[27] H. Le Louarn, J.P. Quere, Les Rongeurs de France: Faunistique et biologie, 2nd edition, *INRA*, 2003.

[28] P.A. Marshall, J.M. Hughes, R.H. Williams, J.E. Smith, R.G. Murphy, G. Hide, Detection of high levels of congenital transmission of Toxoplasma gondii in natural urban populations of Mus domesticus, *Parasitology* 128, 39-42, 2002

[29] N.E. Mateus-Pinilla, B. Hannon, R.M. Weigel, A computer simulation of the prevention of the transmission of Toxoplasma gondii on swine farms using a feline T. gondii vaccine. *Preventive Veterinary Medicine*, 55, 15-26, 2002

[30] J. Montoya, O. Liesenfeld, Toxoplasmosis, *Lancet*, 363, 1965-1976.

[31] E. Nelson, Dynamical Theories of Brownian motion, *Princeton University Press*, 1967.

[32] M.R. Owen, A.J. Trees, Vertical transmission of Toxoplasma gondii from chronically infected house (Mus musculus) and field (Apodemus sylvaticus) mice determined by polymerase chain reaction, *Parasitology* 116, 299-304, 1998.

[33] A.M. Tenter, A.R. Heckeroth, L.M. Weiss, Toxoplasma gondii: from animals to humans, *International Journal for Parasitology*, 31(2), 217-220, 2000.

[34] M. Turner, S. Lenhart, B. Rosenthal, X. Zhao, Modeling effective transmission pathways and control of the world's most successful parasite, *Theoretical Population Biology*, 86, 50-61, 2013.

[35] A. Twomey, On the Stochastic Modelling of Reaction-Diffusion Processes, *eprints.maths.ox.ac.uk*, 2007.

[36] P. van den Driessche, J. Watmough, Reproduction numbers and sub-threshold endemic equilibria for compartmental models of disease transmission, *Mathematical Biosciences* 180, 29-48, 2002.

[37] N. Van Kampen, Stochastic processes in chemistry and physics, 3rd ed, *North-Holland* , 2007.

[38] M. Von Smoluchowski, Zur kinetischen theorie der brownschen molekularbewegung und der suspensionen, *Annalen der Physik*, 326(14): 756-780, 1906.

[39] A. Vyas, S. Kim, N. Giacomini, J.C. Boothroyd, R.M. Sapolsky, Behavioral changes induced by toxoplasma infection of rodents are highly specific to aversion of cat odors, *National Academy of Sciences* 104(15), 6442-6447, 2007.

[40] R.H. Williams, E.K. Morley, J.M. Hughes, P. Duncanson, R.S. Terry, J.E. Smith, G. Hide, High levels of congenital transmission of Toxoplasma gondii in longitudinal and cross-sectional studies on sheep farms provides evidence of vertical transmission in ovine hosts, *parasitology* 130(Pt3):301-7 (2005)

[41] L. Wolpert, R. Beddington, T. Jessel, P. Lawrence, E. Meyerowitz, and J. Smith, Principles of Development, *Oxford University Press*, 2002.